POLITECNICO DI TORINO

Master's Degree in Biomedical Engineering

Master's Degree Thesis

Upper Limb Functional Assessment in PwMS: a MR Paradigm

Supervisors

Prof. Carlo FERRARESI

Prof. Giacinto BARRESI

Anna BUCCHIERI, PhD

Andrea LUCARONI, MsC

Candidates

Miriam MOSCHETTA

Etty SABATINO

Academic year: 2023 - 2024

Abstract

The assessment and rehabilitation of upper limb functionality are crucial aspects to investigate for effectively addressing motor disorders in individuals with neurological impairments. Traditional methodologies lack effective tools for quantifying motor disability, making it difficult to distinguish between pathological movements and normal behaviors.

This Master's Thesis, conducted in collaboration with the Rehab Tecnologies Lab at Italian Institute of Technology (IIT) and Associazione Italiana Sclerosi Multipla (AISM), aims to explore a novel method for evaluating upper limb motor control using a mixed reality (MR) approach with Microsoft HoloLens2, a head-mounted display designed for delivering interactive virtual elements in the area around the user.

The primary goal of this research is to extract, process, and compare data from pathological subjects with those of healthy individuals to identify personalized rehabilitative exercises through interaction with physical objects. Leveraging the hand and eye tracking capabilities of the HoloLens2 device, the study compares kinematic data from healthy subjects and individuals with Multiple Sclerosis, collected during a pick-and-place task in the transverse plane. The task consists of six different movements in the four cardinal directions, delivered in random order. These data are subsequently analyzed to extract metrics related to hand kinematics (morphology, smoothness and efficiency) and hand-eye coordination, to obtain an overall evaluation of movement quality. Comparing metrics from healthy and pathological subjects provides key insights into the differences in motor control and coordination between the two groups, playing a fundamental role in understanding the impact of MS on upper limb functionality.

The secondary goal of the Thesis is to utilize the obtained metrics to identify motor patterns among all analyzed subjects by investigating different classification methods. The results obtained from clustering divide the subjects into four classes: subjects without tremor, subjects with moderate tremor or other cerebellar impairments, subjects with severe tremor, and healthy subjects or those with kinematic behavior similar to that of healthy individuals.

Despite encountered limitations, the results demonstrated the practical usability of HoloLens2 in assessing upper limb impairment levels and underscored the importance of defining personalized rehabilitative protocols to make the recovery of individuals with MS as effective as possible, thereby improving their quality of life.

Abstract

La valutazione e la riabilitazione della funzionalità degli arti superiori, sono aspetti fondamentali da investigare per affrontare efficacemente i disturbi motori in soggetti con disturbi neurologici. Le metodologie tradizionali mancano di strumenti in grado di quantificare efficacemente la disabilità motoria, rendendo difficile la distinzione tra movimenti patologici e comportamenti normali.

Questa Tesi Magistrale, condotta in collaborazione con il Rehab Technologies Lab presso l'Istituto Italiano di Tecnologia (IIT) e l'Associazione Italiana Sclerosi Multipla (AISM), si pone l'obiettivo di esplorare un nuovo metodo di valutazione del controllo motorio degli arti superiori mediante l'utilizzo di un approccio di realtà mista (MR) con Microsoft HoloLens2, un display head-mounted progettato per offrire elementi interattivi nell'area intorno all'utente.

Lo scopo primario della ricerca è quello di estrarre, processare e comparare i dati dei soggetti patologici con quelli dei sani al fine di individuare esercizi riabilitativi personalizzati sfruttando l'interazione con oggetti fisici. Sfruttando le capacità di tracking di mano ed occhio del dispositivo HoloLens2, lo studio vuole mettere a confronto dati cinematici provenienti da soggetti sani e soggetti affetti da Sclerosi Multipla, acquisiti durante un task di pick and place nel piano trasversale. Il task si compone di 6 differenti movimenti nelle 4 direzioni cardinali, erogati in maniera randomica. Questi dati vengono successivamente analizzati per estrarre metriche riguardanti la coordinazione mano-occhio, la morfologia, la fluidità e l'efficienza dei movimenti necessari per ottenere una valutazione complessiva della qualità del movimento. La comparazione delle metriche provenienti da soggetti sani e patologici fornisce degli aspetti chiave riguardanti le differenze nel controllo motorio e nella coordinazione tra i 2 gruppi svolgendo un ruolo fondamentale nel capire l'impatto della Sclerosi Multipla sulla funzionalità degli arti superiori.

Lo scopo secondario della Tesi è quello di sfruttare i risultati ottenuti dalle metriche per identificare dei pattern motori tra tutti i soggetti analizzati indagando differenti metodi di classificazione. I risultati ottenuti dalla clusterizzazione suddividono i soggetti in 4 classi: soggetti senza tremore, soggetti con tremore moderato o altri impairment cerebellari, soggetti con tremore severo e soggetti sani o con comportamento cinematico simile a quello dei sani.

Nonostante i limiti riscontrati, i risultati ottenuti dimostrano l'effettiva usabilità di hololens2 nella valutazione del livello di impairment degli arti superiori e sottolineano l'importanza di definire dei protocolli riabilitativi personalizzati al fine di rendere il recupero dei soggetti affetti da Sclerosi Multipla il più efficace possibile, migliorando la loro qualità di vita.

Acknowledgements

Table of Contents

List of Tables

List of Figures

Acronyms

ADL

Activities of Daily Living

AISM

Associazione Italiana Sclerosi Multipla

AR

Augmented Reality

CNS

Central Nervous System

CSF

Cerebrospinal Fluid

EDSS

Expanded Disability Status Scale

HMDs

Head-Mounted Displays

IMU

Inertial Measurement Unit

IR

Infrared

MRI

Magnetic Resonance Imaging

MS

Multiple Sclerosis

MT

Movement Time

N0C_GA

Gaze Accuracy Number of Zero Crossing Points

NVP

Number of Velocity Peaks

PPMS

Primary Progressive Multiple Sclerosis

PRMS

Progressive-Relapsing Multiple Sclerosis

PwMS

People with Multiple Sclerosis

RRMS

Relapsing-Remitting Multiple Sclerosis

SPARC

Spectral Arc Length

SPMS

Secondary Progressive Multiple Sclerosis

VEP

Visual Evoked Potentials

VR

Virtual Reality

XR

Mixed Reality

Chapter 1

Introduction

Upper-limb impairments are a common consequence of various neurological disorders, significantly affecting the functional independence and quality of life of individuals. Accurate assessment of upper-limb function is crucial for diagnosing these conditions, guiding treatment, and monitoring recovery. The upper limbs play a vital role in performing daily activities and engaging in social and occupational tasks. Neurological disorders such as stroke, multiple sclerosis (MS), cerebral palsy, and traumatic brain injury often result in deficits in motor control, coordination, strength, and dexterity of the upper limbs. Evaluating these impairments is essential for developing personalized rehabilitation strategies and optimizing therapeutic outcomes.

The development of motor skills is essential for enabling individuals to interact effectively with their environment and perform complex activities that require comprehensive body coordination. The musculoskeletal system, which includes bones, joints, and muscles, operates as a kinetic chain, where movement in one segment influences the entire body [1]. Individuals with neurological disorders experience significant disruptions in their kinetic and kinematic behaviors, which affect both fundamental and functional movements, leading to impairments in upper-limb motor abilities that can profoundly impact a person's independence and mental health [2]. Neurological patients typically undergo specialized treatments administered by physiotherapists, with the intensity of these treatments varying based on the stage of recovery. For those with upper-limb impairments, initial treatment often requires full assistance to perform basic movements. As motor functions improve, patients transition to partial assistance, eventually progressing to home-based rehabilitation during the chronic stage. To effectively tailor these treatments and monitor progress, various methodologies for assessing upper-limb impairment in patients with neurological disorders have been developed.

1.1 Upper-Limb Assessment in Neurological Disorders

Clinical assessments are among the most widely used tools for evaluating upper-limb function. These assessments involve standardized tests and observational checklists that measure various aspects of motor performance. Notable clinical assessments include:

- **The Nine-Hole Peg Test (NHPT)**: As highlighted by the International Journal of Rehabilitation Research (1981) [3], the NHPT is a standardized assessment tool widely used to measure fine motor coordination and dexterity of the upper limbs. The test involves timing the patients as they place nine pegs into nine holes on a pegboard and then remove them (Figure 1.1). This process provides a quantitative measure of hand function, which is particularly useful for evaluating motor impairment in individuals with neurological disorders. In clinical practice, the time taken to complete the NHPT is typically measured in seconds. The results can be interpreted as follows: a shorter completion time indicates better motor function of the upper limbs, characterized by faster peg manipulation and removal. Conversely, a longer completion time reflects greater motor impairment, with reduced speed of execution and potential difficulties in coordination and motor precision.
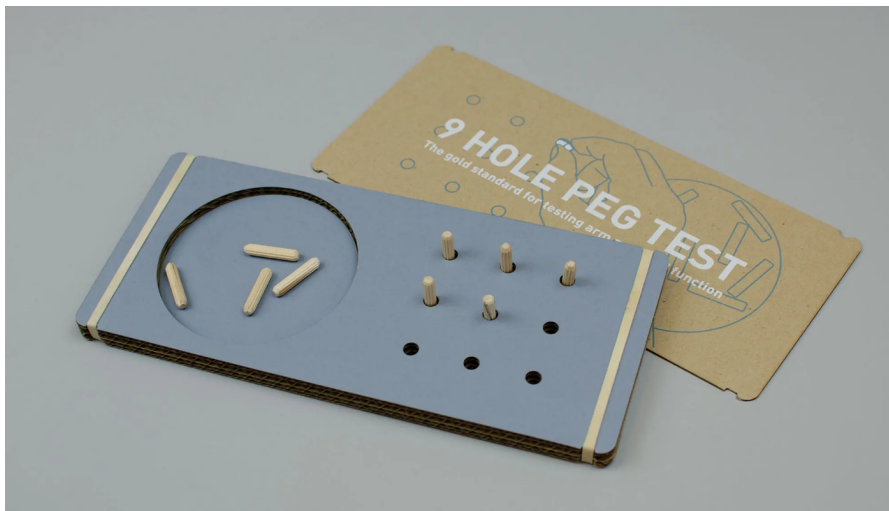
Figure 1.1: Nine-Hole Peg Test equipment

- **The Manual Muscle Test (MMT)**: This test evaluates muscle strength by having patients resist manual force applied by the examiner [4]. It is

particularly useful for assessing the degree of muscle weakness in patients with neurological disorders.

- **The Expanded Disability Status Scale (EDSS)**: This method is used to quantifiy the disability level in people with multiple sclerosis (PwMS). It assesses a range of neurological functions, including muscle strength, coordination, speech, swallowing, sensory functions, and bowel and bladder control. The scale ranges from 0 to 10, with increments of 0.5. Lower scores (0 to 4.5) reflect minimal to moderate disability with retained ambulatory ability, while higher scores (5.0 to 9.5) indicate increasing levels of disability and reduced walking ability (Figure 1.2). EDSS is widely used in clinical trials and by neurologists to monitor disease progression and evaluate the effectiveness of treatments [5].
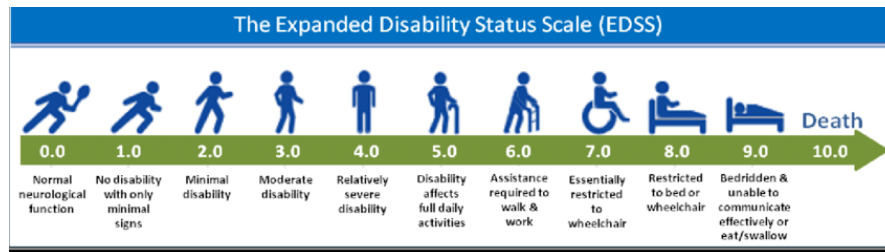
Figure 1.2: Expanded Disability Status Scale

- **The Fugl-Meyer Assessment (FMA)**: This comprehensive assessment tool is a widely used clinical tool designed to assess motor function, balance, sensation, and joint functioning in individuals who have experienced a stroke. It includes subtests for upper-limb motor function, coordination, and reflex activity, offering a detailed profile of motor impairment. It is particularly valuable in rehabilitation settings to evaluate the recovery of motor skills and to track progress over time [3].

- **The Box and Block Test (BBT)**: It is a standardized assessment tool designed to measure manual dexterity, particularly in the context of upper-limb function. During the test, the individual is asked to transfer as many small blocks as possible from one compartment of a box to another within a set time frame, typically one minute (Figure 1.3). The number of blocks successfully transferred serves as a quantitative measure of hand dexterity and motor coordination. A higher score, indicating more blocks transferred, suggests better manual dexterity and upper-limb function. Conversely, a lower score reflects greater difficulty in manual tasks, potentially due to impaired motor skills. The BBT is particularly valued for its sensitivity in detecting

changes in hand function over time, making it a valuable tool for assessing treatment outcomes and guiding rehabilitation strategies [6].

Figure 1.3: Box and Block Test equipment

Instrumental assessments utilize advanced technologies to provide objective and quantitative data on upper-limb function, capturing subtle changes in motor performance that may not be evident through clinical assessments alone. Among the most widely used methods of instrumental assessment, we can include:

- **Motion Capture Systems**: Motion capture systems are advanced technological tools used to accurately capture and analyze human movement. They employ various sensors, markers, or cameras to track the position and orientation of body segments or joints in three-dimensional space. These systems provide precise measurements of joint angles, movement trajectories, and timing during functional tasks. This data is crucial for understanding motor impairments, evaluating rehabilitation progress, and guiding personalized treatment plans for individuals with neurological disorders or other conditions affecting upper-limb function [7].

- **Electromyography (EMG)**: EMG measures muscle electrical activity during contraction, providing insights into muscle activation patterns and neuromuscular control. This method is valuable for understanding the underlying mechanisms of motor impairments and guiding targeted interventions [8].

Recent advancements in technology have led to the development of innovative assessment tools that enhance the accuracy and reliability of upper-limb evaluations. Virtual Reality (VR) and Augmented Reality (AR) environments offer immersive and interactive platforms for assessing and rehabilitating upper-limb function. These technologies can simulate real-life tasks and provide real-time feedback, making the assessment process engaging and effective. Additionally, wearable sensors, such as inertial measurement units (IMUs) and accelerometers, enable continuous monitoring of upper limb movements in naturalistic settings. They offer valuable data on movement quality and patterns over extended periods, providing a more comprehensive assessment of motor function [7].

Accurate assessment of upper-limb function is crucial for the effective management of neurological disorders. A combination of clinical, instrumental, and patient-reported outcome measures offers a comprehensive evaluation of upper-limb impairments, guiding personalized rehabilitation strategies. Advances in technology continue to enhance the precision and scope of these assessments, promising improved outcomes for individuals with neurological conditions.

1.2   Multiple Sclerosis

Multiple sclerosis (MS) is a chronic autoimmune disease that primarily affects the central nervous system (CNS), encompassing the brain and spinal cord. Typically diagnosed in young adults aged 20 to 50, MS impacts approximately 2.8 million people worldwide (130.000 in Italy, with an incidence of about 3400 cases per year), with varying prevalence geographically, indicating potential environmental influences such as sunlight exposure. Other suspected risk factors include viral infections like the Epstein-Barr virus, genetic predisposition, and possibly specific dietary factors and deficiencies, notably vitamin D [9].

The disease is characterized by inflammation, demyelination (the breakdown of the protective myelin sheath around nerve fibers), and, in some cases, axonal injury (Figure 1.4). This disruption impairs nerve signal transmission in the CNS, leading to a diverse range of neurological symptoms.

Common manifestations of MS include optic neuritis causing visual disturbances, muscle weakness and spasticity, challenges with coordination and balance, sensory issues such as paresthesias, bladder and bowel dysfunction, chronic fatigue, and cognitive and mood impairments. Symptoms may follow a relapsing-remitting pattern of intermittent exacerbations and remissions or a progressive course with gradual deterioration over time [10].

Diagnosis of MS relies on a combination of clinical criteria, magnetic resonance imaging (MRI), cerebrospinal fluid (CSF) analysis, and visual evoked potentials
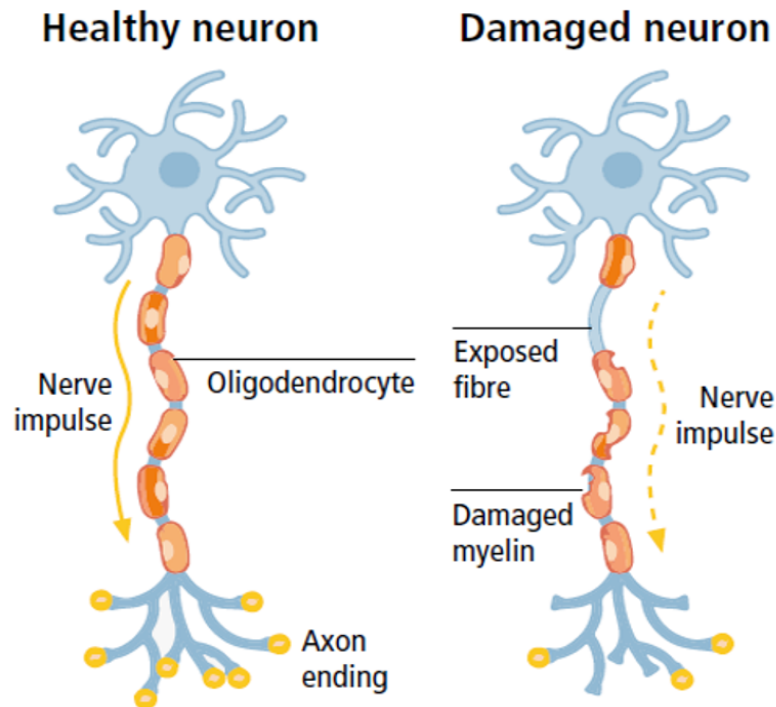
Figure 1.4: Comparison between a healthy neuron and a damaged neuron. The healthy neuron on the left shows a normal nerve impulse transmission along the axon, facilitated by intact myelin sheaths. The damaged neuron on the right exhibits disrupted nerve impulse transmission due to damaged myelin and exposed nerve fibers.

(VEP) testing.

MRI remains the cornerstone for diagnosing MS, as it can reveal characteristic lesions in the CNS that are crucial for accurate diagnosis [11]. Advanced MRI techniques, such as diffusion tensor imaging and functional MRI, have enhanced our ability to detect subtle changes in brain tissue, offering valuable insights into disease progression and the efficacy of therapeutic interventions. In addition to MRI, CSF analysis can reveal the presence of oligoclonal bands, which are indicative of chronic inflammation within the CNS and further corroborate the diagnosis of MS. VEP tests measure the brain's electrical activity in response to visual stimuli, with abnormalities often pointing to demyelination of the optic pathways, a common manifestation in MS. These diagnostic tools, when utilized together, significantly improve the accuracy of MS diagnosis and enable more effective monitoring of disease progression and treatment responses.

The McDonald criteria, introduced in 2001 and revised in 2017, are fundamental in confirming MS diagnosis, emphasizing the dissemination of lesions in both time and space within the CNS. These criteria require evidence of:

- Dissemination in time, demonstrated by the occurrence of new lesions or clinical relapses over time.

- Dissemination in space, indicated by lesions observed in different CNS locations, typically detected through MRI.

In addition to these radiological and clinical markers, the McDonald criteria also incorporate other diagnostic tests to exclude alternative diagnoses and confirm MS [12].

Integrating these criteria enables clinicians to effectively classify MS into its different forms:

- **Relapsing-Remitting MS (RRMS)**: Characterized by episodic acute attacks followed by partial or complete recovery periods.

- **Secondary Progressive MS (SPMS)**: Initially presents as RRMS, transitioning to a more progressive course with accruing disability over time.

- **Primary Progressive MS (PPMS)**: Features a steady decline in neurological function from the disease's onset, without distinct relapse and remission phases.

- **Progressive-Relapsing MS (PRMS)**: A rare subtype with continuous disease progression alongside acute exacerbations [10].

Accurate diagnosis and classification of MS are essential for initiating timely and appropriate treatment strategies tailored to the specific clinical course of the disease.

1.2.1 Impact of MS on Activities of Daily Living

MS has a substantial impact on an individual's capacity to perform Activities of Daily Living (ADLs). These activities encompass essential self-care tasks such as eating, dressing, and bathing, as well as more complex activities like managing finances, driving, and household maintenance. The degree of impact varies depending on the progression of the disease and the specific symptoms experienced by the individual.

A primary symptom of MS is fatigue, which affects most patients and can be debilitating. Fatigue in MS is often described as overwhelming and not necessarily linked to physical exertion [13]. This severe fatigue can significantly restrict an

individual's ability to perform daily tasks, thus diminishing their quality of life. For instance, an individual with MS may find it exhausting to complete simple tasks such as brushing their teeth or preparing a meal, resulting in increased reliance on others.

Motor dysfunction is another critical aspect of MS that affects ADLs. MS can cause muscle weakness, spasticity, and coordination problems, making movements difficult and often painful. Tasks requiring fine motor skills, such as buttoning a shirt or writing, can become especially challenging. Moreover, balance and gait issues common in MS increase the risk of falls, complicating walking, climbing stairs, and other mobility-related activities.

Cognitive impairments associated with MS also significantly impact ADLs. Many individuals with MS experience difficulties with memory, attention, and executive functions [14]. These cognitive challenges can complicate the planning and execution of daily activities. For example, an individual with MS might struggle to remember steps in a recipe, manage medications, or keep track of appointments, necessitating additional support and adaptive strategies.

Sensory disturbances are prevalent in MS and can include numbness, tingling, and pain. These sensory issues can interfere with the ability to feel and manipulate objects, further complicating daily tasks [10, 15]. For instance, numbness in the hands can make it difficult to grasp utensils, turn doorknobs, or use a computer keyboard, affecting both personal and professional aspects of life.

Visual disturbances, such as double vision, blurred vision, and vision loss, also impact ADLs [16]. These visual problems can make it challenging to read, drive, and navigate environments safely. Even with corrective lenses, the fluctuating nature of MS symptoms can lead to inconsistent visual capabilities, requiring adaptive strategies and tools to manage daily activities effectively.

Depression and anxiety, often comorbid with MS, further exacerbate difficulties with ADLs. The emotional burden of living with a chronic illness can reduce motivation and energy, impacting one's ability to engage in self-care and maintain social relationships. Psychological support and interventions are crucial in helping individuals with MS manage these emotional challenges and improve their overall functioning.

MS affects ADLs through a complex interplay of physical, cognitive, sensory, and emotional symptoms. The impact is multifaceted, necessitating comprehensive management strategies that include medical treatment, rehabilitation, adaptive devices, and psychological support. Understanding the various ways MS influences daily life is essential for developing effective interventions that enhance independence and quality of life for individuals living with this condition.

1.2.2 Movement disorders in Multiple Sclerosis

Patients with MS could exhibit cerebellar symptoms, including tremor, ataxia, imbalance, and speech disturbances. Clinical examinations may reveal intention tremor (dysmetria), head titubation, truncal ataxia, and nystagmus, which suggest cerebellar or cerebellovestibular dysfunction. Speech can become scanning or explosive. Distinguishing pure cerebellar dysfunction is challenging due to overlaps with motor, sensory, and cerebral impairments. Truncal ataxia, frequently resulting from multiple lesions, is exacerbated by proprioceptive loss from posterior column involvement. Although cerebellar signs are rare in clinically isolated syndrome (CIS), they are more prevalent in early-onset MS [17]. A comprehensive analysis of some of these movement disorders in MS will further elucidate their complexities and impact on patients.

1. **Cerebellar tremor**: it is a clinical manifestation characterized by rhythmic, involuntary oscillations of the limbs, primarily due to cerebellar dysfunction. This type of tremor is distinct from more common forms, such as essential tremor or parkinsonian tremor, with unique features and specific pathophysiological implications. In patients with multiple sclerosis (PwMS), cerebellar tremor often forms part of a complex motor disorder that also includes dysmetria and ataxia-related symptoms [18].

   Various types of tremor exist, including resting tremor, action tremor, which can be further categorized as postural (when the limb is held against gravity), kinetic (during movement), and intentional (at the end of a purposeful movement). In multiple sclerosis (MS), tremor is prevalent, affecting 25% to 58% of patients [19].

   A particularly prevalent subtype of cerebellar tremor in PwMS is intentional tremor, which significantly impairs upper limb function. This tremor manifests or worsens during voluntary movements aimed at a target, such as reaching or pointing. The pathophysiology of intentional tremor in MS involves cerebellar lesions or disruptions in its pathways, resulting in compromised coordination and muscle activity timing [20].

   The frequency characteristics of cerebellar tremor vary; studies by Hess and Pullman (2012) [21] and Labiano-Fontcuberta and Benito-Leoen (2018) [22] report tremor frequencies ranging between 4-12 Hz. Additionally, research by Wurster et al. (2017) [23] indicates that most frequency components of cerebellar tremor are concentrated between 3 and 5 Hz. This variability highlights the underlying cerebellar dysfunction, which hampers precise movement control and limb stabilization.

   Cerebellar tremor severely impacts ADL, such as writing or eating, creating substantial challenges to the patient's quality of life. The inability to maintain

a stable posture or perform precise movements often results in frustration and significant functional limitations. Addressing cerebellar tremor, particularly intentional tremor, is essential for enhancing daily living activities and overall well-being in PwMS [20].

2. **Ataxia**: Ataxia is a prevalent and disabling condition in patients with multiple sclerosis (MS), primarily resulting from damage to the cerebellum or its pathways. This disorder impairs motor coordination and can affect the limbs, trunk, and speech. Common symptoms include dysmetria, where patients misjudge the distance or range of movements, dysdiadochokinesia, characterized by difficulty in performing rapid alternating movements, and nystagmus, which involves involuntary eye movements. Patients with ataxia often display a wide-based, unstable gait, necessitating slower and shorter strides for stability. Additionally, ataxic speech is marked by altered rate, prosody, and modulation, leading to clumsy and irregular speech patterns. Coordination of eye movements is frequently disrupted, resulting in nystagmus and hypometric or hypermetric saccades. The underlying pathology typically involves lesions in the cerebellum or cerebellar projections to the brain, brainstem, thalamus, and spinal cord. Midline cerebellar lesions are associated with truncal ataxia and gait instability, whereas unilateral limb ataxia is usually due to ipsilateral cerebellar hemisphere lesions. Posterior cerebellar lesions can cause balance problems and eye-movement discoordination. Furthermore, ataxia may also result from demyelinating lesions in the midbrain, thalamus, or pericentral gyrus [19]. These diverse manifestations underscore the complexity of ataxia in MS, highlighting the necessity for comprehensive and multidisciplinary management approaches to address the significant long-term disability it causes in patients.

3. **Dystonia**: Dystonia is characterized by abnormal, sustained muscle contractions that result in twisting or repetitive movements around one or more joints. In the context of MS, paroxysmal dystonia, also known as tonic spasms, is the most commonly observed type. Unlike typical dystonia, these spasms involve involuntary contractions of limbs, causing brief, painful posturing or movements that can occur multiple times a day. Cervical dystonia, or spasmodic torticollis, is another form of dystonia occasionally observed in MS patients. It affects the muscles of the neck, resulting in abnormal head movements and sustained, often painful postures of the head, neck, and shoulders. While some consider cervical dystonia and MS to be coincidental, recent case reports suggest a potential causative relationship, supported by lesions in the cervical spine [19].

4. **Dysarthria**: it is a motor speech disorder characterized by difficulty artic-
   ulating words due to weakness or incoordination of the muscles involved in
   speech production. It typically results from lesions or dysfunction in the
   nervous system, affecting areas such as the brainstem, cerebellum, or motor
   cortex. Individuals with disartria may experience slurred speech, imprecise
   pronunciation, and difficulties controlling the rate, rhythm, and volume of
   speech. Treatment approaches often focus on improving speech clarity through
   speech therapy techniques tailored to address specific underlying neurological
   deficits [17].

1.2.3   Hand-Eye Coordination in PwMS

Eye-hand coordination represents a particularly challenging aspect affected by
cerebellar tremor, crucial for tasks requiring intricate motor control. Cerebellar
tremor detrimentally affects visual tracking and precise targeting of specific spatial
locations.

The compromise in eye-hand coordination among individuals with cerebellar
tremor is evident in their struggles with visual tracking and performance of compli-
cated motor tasks. Quantitative assessment of this impairment involves specific
tests evaluating the patient's capacity to coordinate eye and hand movements in
response to visual or tactile stimuli.

A study by Brown et al. (1996) [24] elaborates on the disruption of eye-
hand coordination in PwMS, noting significant delays in initiating and executing
coordinated movements. This delay can be attributed to demyelination and axonal
damage in neural pathways connecting the cerebellum and motor cortex, which are
critical for synchronized motor activities.

Feys et al. (2003) [25] further investigated the impact of cerebellar tremor
on upper limb function, highlighting that the severity of tremor correlates with
the degree of impairment in eye-hand coordination. Their findings suggest that
therapeutic interventions aimed at reducing tremor amplitude could potentially
improve coordination and functional independence.

Moreover, the incorporation of cutting-edge technologies like motion capture
systems and virtual reality (VR) platforms presents promising opportunities to
evaluate and rehabilitate eye-hand coordination, as it can simultaneously provide
eye-tracking and hand-tracking data. These advancements offer immediate feedback
and adaptive training environments, potentially improving motor learning and the
development of compensatory techniques [26].

Prompt detection and efficient treatment of cerebellar tremor are crucial to
enhance patients' quality of life and minimize negative effects on both motor and

cognitive functions. Customized rehabilitation regimens aimed at improving eye-hand coordination can significantly contribute to preserving functional autonomy and overall health in individuals affected by multiple sclerosis.

1.3 Virtual Reality, Augmented Reality and Mixed Reality in Rehabilitation

Impairments in upper limb function significantly impact an individual's ability to perform daily activities, diminishing autonomy and affecting mental well-being. Effective treatment is crucial for individuals with neurological conditions, such as stroke survivors and those with multiple sclerosis, to regain or maintain independence in daily tasks.

Occupational therapy is designed to optimize functional recovery through specialized interventions, typically administered in clinical environments. Encouraging active patient involvement is crucial for fostering neuroplasticity and maintaining therapeutic gains over time [27]. Personalized feedback, whether visual, auditory, or tactile, plays a key role in enhancing patient engagement during rehabilitation sessions. The integration of immersive technologies enhances the therapeutic environment, potentially improving treatment outcomes [28, 29]. The following section outlines various forms of immersive technologies—Virtual Reality (VR), Augmented Reality (AR), and Mixed Reality (MR)—and their utilization in rehabilitation, particularly in developing personalized exergames tailored to individual patient requirements [30].

- **Virtual reality (VR)** has transformed rehabilitation by offering immersive environments that simulate real-life scenarios and therapeutic activities. [31] VR experiences, facilitated through head-mounted displays (HMDs) with optional haptic feedback, provide a safe environment for patients, such as stroke survivors, to practice and refine motor skills.

- **Augmented reality (AR)** enhances the user's perception of their physical environment by overlaying digital information onto real-world scenes. This technology can be accessed through devices such as smartphones, tablets, or AR glasses. In rehabilitation settings, AR offers real-time guidance and feedback during exercises. For example, patients can receive virtual prompts and corrections superimposed on their actual movements, aiding in more precise and effective exercise performance.

- **Mixed reality (MR)** integrates elements of both virtual reality (VR) and AR, enabling interaction between virtual and real objects. Devices like the *Microsoft HoloLens 2* allow users to visualize and interact with holographic images within

their physical surroundings. In rehabilitation, MR enables interactive therapy sessions where patients engage with virtual objects during exercises, obtaining instant feedback on their performance. This hybrid approach combines real-world elements with virtual elements, enhancing the dynamic and personalized nature of rehabilitation exercises tailored to individual patient needs.

The incorporation of AR and MR technologies in rehabilitation presents advantages over traditional VR methods, particularly in enhancing hand-eye coordination through interactive games. VR and AR technologies have been widely implemented in the field of motor recovery, demonstrating their efficacy in clinical settings. In contrast, MR applications, as highlighted in recent studies [31], are progressively gaining recognition and acceptance for their potential to revolutionize rehabilitation practices. These technologies enable the creation of personalized and interactive environments tailored to the specific needs of patients, utilizing cameras, sensors, and additional instruments for biometric measurements such as hand tracking and eye-tracking. The Microsoft HoloLens 2 exemplifies this capability, particularly suited for simulating daily living environments.

Patient engagement stands as a crucial determinant in the efficacy of rehabilitation programs [32]. Conventional rehabilitation exercises often suffer from monotony and repetition, which can lead to decreased motivation and adherence. MR addresses this challenge by offering immersive and stimulating experiences that make rehabilitation activities more enjoyable. This enhanced engagement encourages patients to actively participate consistently in their therapy. In MR-based rehabilitation, patients interact with virtual objects and projections, engaging in a wide spectrum of activities ranging from simple exercises to complex, task-oriented scenarios. These virtual elements are designed to provide immediate feedback, rewards, and progress tracking, fostering further motivation and involvement. By transforming therapy sessions into interactive and enjoyable experiences, MR has the potential to enhance patient compliance and ultimately improve rehabilitation outcomes.

1.3.1 Head-Mounted Visors using AR and MR for rehabilitation programs

Motion capture (mocap) techniques have undergone substantial evolution, enabling the precise and detailed measurement of limb movements in various applications. Recent advancements in augmented reality (AR) and mixed reality (MR) technologies have introduced head-mounted visors as a state-of-the-art tool for motion capture [7]. Devices like the Microsoft HoloLens 2 seamlessly integrate AR/MR capabilities with advanced motion tracking functionalities, presenting a range of significant advantages:

- **Markerless Tracking**: Head-mounted visors utilize internal sensors and cameras to monitor upper limb movements without the requirement for reflective markers, enhancing user comfort and operational ease.

- **Enhanced Interaction**: AR/MR environments overlay digital data onto the real-world environment, facilitating interactive and immersive rehabilitation exercises and training scenarios. This feature enhances patient engagement and allows for dynamic therapy sessions.

- **Portability and Convenience**: These devices are compact and simple to deploy, making them adaptable for diverse settings, including clinical facilities and patients' homes.

These technological advancements in AR and MR not only enhance the precision of motion capture but also broaden the scope of rehabilitative interventions by integrating digital elements seamlessly into physical therapy environments.

Nevertheless, head-mounted visors encounter several challenges that warrant consideration. One notable concern is the potential for reduced accuracy in capturing intricate limb movements, particularly those involving fine motor skills or performed outside camera tracking area. This limitation could affect the precision required for detailed rehabilitation assessments and interventions.

Furthermore, the restricted field of view inherent in these devices may hinder patient engagement during therapy sessions. This limitation could impact the user's ability to interact fully with virtual elements or complete tasks that require a broader visual perspective.

Another critical factor is the limited battery life of head-mounted visors, which imposes constraints on their practical use in both clinical and research settings. Prolonged therapy sessions or extensive data collection periods may necessitate frequent recharging, potentially disrupting the continuity and efficiency of rehabilitation practices.

Addressing these challenges through ongoing technological advancements and ergonomic design improvements remains essential to maximize the effectiveness and user acceptance of head-mounted visors in rehabilitation applications. Efforts to enhance motion capture accuracy, expand the field of view, and optimize battery performance are fundamental in ensuring these devices contribute positively to therapeutic outcomes and patient experiences.

1.4 Objectives

This master's thesis focuses on advancing the rehabilitation of upper-limb function critical for PwMS. Accurately assessing treatment progress is crucial for tailoring personalized therapy, yet current methods rely largely on subjective clinical evaluations.

Collaborating with the Italian Institute of Technology, this study explores the potential of the Microsoft HoloLens 2, a mixed-reality head-mounted display, as an innovative tool for assessing upper-limb functionality in rehabilitation settings. The research emphasizes HoloLens2's capability to offer a portable and cost-effective solution by utilizing its advanced sensors for quantitative hand and eye-tracking data collection.

The study employs HoloLens2's ROCKapp application, which integrates holographic elements with physical objects to assess pick-and-place task performance crucial for upper-limb rehabilitation. By analyzing these tasks, the research aims to derive clinically relevant kinematic data metrics such as movement quality, coordination and movement accuracy. These metrics promise to provide more precise assessments of patient progress.

A primary objective of this research is to enable clinicians to make informed comparisons between healthy individuals and MS patients, thereby strengthening their understanding of upper-limb impairments and facilitating tailored interventions.The integration of immersive technology through Microsoft HoloLens2 not only enhances assessment accuracy but also offers potential therapeutic benefits, such as improving patient engagement, providing real-time feedback to enhance motor learning, and creating personalized and interactive therapy sessions tailored to individual patient needs. In this way, this thesis aims to contribute to the development of more effective and personalized rehabilitation strategies, aiming to improve the quality of life for individuals living with MS.

Chapter 2

Materials and methods

This study explores the use of Microsoft HoloLens2, an advanced mixed-reality head-mounted display, as a cutting-edge alternative to traditional motion capture systems for assessing upper-limb functionality in rehabilitation. HoloLens2 enables precise quantitative recordings of hand movements and fosters patient engagement through its ROCKapp application. This application integrates holographic elements with physical objects to evaluate essential pick-and-place tasks for upper-limb rehabilitation, offering a novel approach to interactive therapy sessions. Recent evaluations have demonstrated that the accuracy of HoloLens2's hand-tracking capabilities is comparable to that of traditional motion capture systems, yielding a cross-correlation exceeding 0.95% and a root-mean-square error percentage below 10%. These promising outcomes underscore HoloLens2's attributes as a portable, user-friendly, and cost-effective solution for the precise quantification of hand movements, potentially paving the way for tailored therapeutic interventions [33].

2.1 Microsoft Hololens 2

Microsoft HoloLens 2 is a cutting-edge MR head-mounted display that combines advanced hardware and software to provide an immersive user experience. This device boasts a wide range of specifications and features designed to enhance both consumer and professional applications, including rehabilitation. [34]

- **Design and Ergonomics**: The Microsoft HoloLens 2 combines functionality with user comfort, boasting a sleek, lightweight design that promotes extended wear without discomfort, making it suitable for long-term use in diverse applications. It includes an adjustable headband and a balanced center of gravity, ensuring a comfortable fit for various head sizes and shapes. Moreover, the visor is designed to flip up, allowing users to effortlessly transition between mixed reality and their real-world environment. (Figure 2.1)

16

Figure 2.1: Hololens2 worn by user in flipped up mode

- **Display and Optics**: The Microsoft HoloLens 2 incorporates two high-resolution displays with a combined resolution of 2k per eye, providing a crisp and detailed visual experience. Its custom-built, high-definition holographic lenses offer a wide field of view, enhancing depth and presence. Using transparent holographic optics and waveguides, the device projects digital content directly into the user's view, seamlessly integrating virtual elements with the real world. The display supports high contrast and vibrant colors, ensuring sharp holograms in various lighting conditions. With a sophisticated optical system and rapid refresh rate, motion blur is minimized, enhancing the realism and engagement of the mixed reality content.

- **Sensors and Tracking**: The Microsoft HoloLens 2 incorporates a sophisticated array of sensors for precise tracking and interaction. Head tracking is enabled by four visible light cameras, ensuring accurate spatial awareness and positional tracking. For eye tracking, the device utilizes two infrared cameras (IR), which capture and interpret eye movements to enhance user interaction and control. Depth sensing is facilitated by a time-of-flight depth sensor with a resolution of 1 megapixel, allowing for detailed environmental mapping and object interaction in mixed reality scenarios. Additionally, an inertial measurement unit (IMU) comprising accelerometer, gyroscope, and magnetometer components provides real-time data on the device's orientation and motion. The integrated 8-megapixel camera supports high-resolution still

images and 1080p30 video recording, enhancing the device's capability for capturing and sharing mixed reality experiences (Figure 2.2).
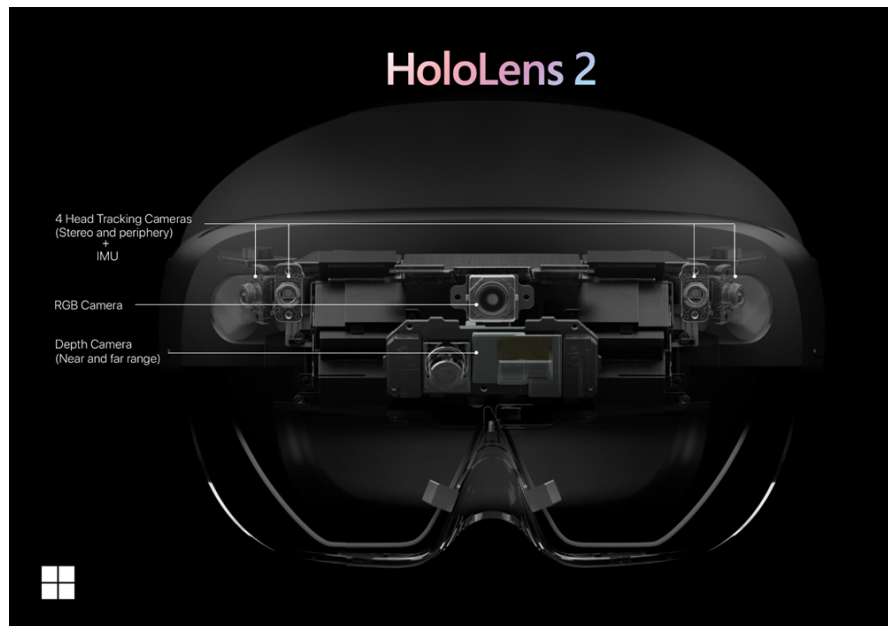
Figure 2.2: Hololens 2 sensors front view

- **Computing Power**: The Microsoft HoloLens 2 harnesses the computational prowess of a custom Qualcomm Snapdragon 850 processor, meticulously engineered to meet the exacting requirements of mixed reality applications. This powerful processor ensures seamless performance and responsiveness, allowing the device to process complex holographic images and interactive elements in real-time. Coupled with 4 GB of RAM and 64 GB of storage, the HoloLens 2 can run multiple applications simultaneously without compromising on performance. This robust computing architecture enables users to experience immersive mixed reality environments with minimal latency, enhancing productivity and interaction in various professional and educational settings.

- **Connectivity**: The Microsoft HoloLens 2 is equipped with robust connectivity options, including Wi-Fi 802.11ac and Bluetooth 5.0, ensuring seamless integration into various network environments. These features enable fast data transfer, wireless communication, and connectivity to peripherals, enhancing its versatility in mixed reality applications.

- **User Interface and Interaction**: The Microsoft HoloLens 2 offers an intuitive user interface designed for immersive interaction in mixed reality environments. It supports gaze, gesture, and voice commands, allowing

natural manipulation of holographic elements. Enhanced by eye-tracking and hand-tracking technologies, users can interact with virtual objects simply by looking at them or using hand gestures. The interface is responsive and customizable, facilitating seamless navigation through applications while maintaining awareness of the real-world surroundings.

2.1.1   ROCKapp

ROCKapp leverages Microsoft HoloLens 2 to provide a novel approach to functional MS assessment. This application, designed and implemented by A. Lucaroni at the Rehab Technologies Lab, integrates holographic elements with physical objects and markers to create interactive environments where MS patients can perform specific upper limb tasks, such as pick-and-place exercises. These tasks are crucial for assessing fine motor skills, coordination, and overall upper limb functionality.

The mixed reality (MR) environment was constructed using Unity 2021.2.16f1, with integration of both MRTK and PTC Vuforia extensions. This environment was then projected onto a Microsoft HoloLens2 device.

The MRTK package offers essential components for spatial interactions and user interface elements. This framework equips developers with the necessary APIs to utilize the user's hands as interactive tools. It can accurately compute the position and orientation of each hand joint, including the fingers (with each phalanx), knuckles, palm, and wrist.

PTC Vuforia, an augmented reality (AR) software, enabled holographic interaction by leveraging different image recognition algorithms. Upon detection of specific image targets by the HoloLens2 camera, Vuforia anchored holograms to these targets, enhancing the AR experience [33].

Once started, the user visualizes a holographic target upon which a 500 ml physical bottle is to be placed. A cylindrical PTC Vuforia marker is attached on top of the bottle cap (Figure 2.3).

When recognized by the cameras, HoloLens 2 tracks the image from all directions. The user is expected to move the object based on four different cues positioned as cardinal points: in front close (S), in front distant (N), on the left (W), and on the right (E). Virtual target N is placed in front of the user at a distance of maximum arm extension. S, W, and E coincide with vertices of a square of side 28 cm. Position N serves as a reference upon which the bottle needs to be placed back once moved to either S, W, or E. The order of appearance of these three cues is randomized.

During the task, whenever the user places the object on the activated target, a holographic rocket is launched. Participants are instructed to repeat the task 30 times distributed across 5 trials with 6 movements each. Particularly, Unity Engine's colliders (Figure 2.4) are utilized to detect when either the box or the

Figure 2.3: ROCKapp on HoloLens 2: interactive environment

bottle is picked and when it is placed on the target. The collider, a Unity component invisible to the user, defines object boundaries and calculates collisions in virtual worlds, and its shape can be customized as needed.

In ROCKapp the holographic targets are characterized by a collider (C2), while the bottle is equipped with collider C1. When C1 and C2 intersect, a flag linked to object placement is activated. Simultaneously, when the hand (equipped with collider C2) initially collides with the bottle (C1), a flag connected to object picking is raised.

ROCKapp incorporates several key features that position it as a cutting-edge tool for functional assessment:

- Holographic Integration: ROCKapp seamlessly overlays digital cues onto physical objects and markers in the user's real-world environment, enhancing the assessment experience with intuitive and immersive interactions.

- Real-time Tracking: Leveraging advanced sensors and tracking capabilities of HoloLens 2, ROCKapp accurately captures hand and eye movements during task performance. This real-time data acquisition provides clinicians with objective metrics to assess movement quality and functional limitations.

- Quantitative Analysis: The application records data with annotations useful for processing from hand and eye-tracking sensors to generate quantitative metrics, including movement speed, accuracy, and coordination. These metrics provide valuable insights into disease progression and the effectiveness of rehabilitation interventions.
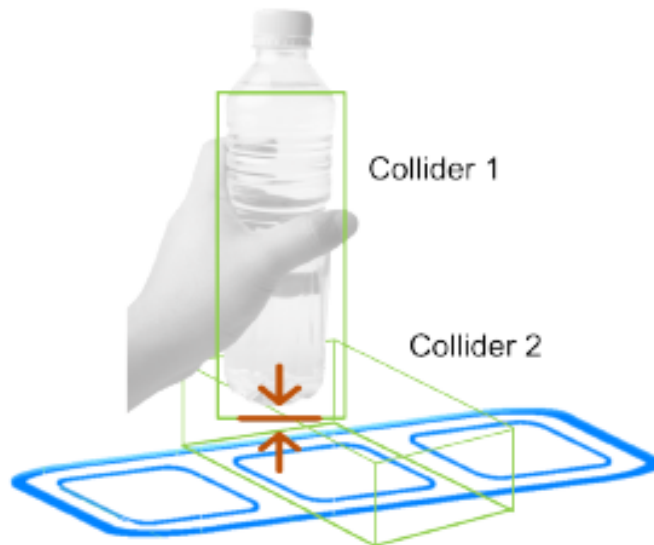
Figure 2.4: Representation Unity colliders for ROCKapp

In clinical settings, ROCKapp serves as a valuable tool for monitoring the progression of MS-related motor impairments and evaluating the impact of therapeutic interventions. By delivering objective and standardized assessments, clinicians can tailor treatment plans to individual patient needs, thereby optimizing rehabilitation outcomes and improving patient quality of life.

2.2   Participants

The study aimed to obtain data from healthy subjects for subsequent calculation and comparison with those of MS patients, in order to obtain a classification method.

The group of healthy subjects comprised 12 individuals, including 4 males and 8 females, with an average age of 42.15 ± 8.13. The age range within this group varied from 28 to 60 years.

The MS group consisted of 9 individuals, including 4 males and 5 females, with an average age of 42.11 ± 12.53 years. The age range within this group varied from 29 to 64 years. PwMS group was characterised by different levels of disability both in the upper and lower limb. In particular, 3 individuals had been diagnosed with cerebellar tremor.

The subjects were classified into four distinct classes based on the analysis of clinical test values from the EDSS, NHPT, and BBT. Class 1 consisted of individuals with MS but without cerebellar impairments. Class 2 included MS

subjects with cerebellar impairments or moderate tremor. Class 3 comprised MS patients experiencing severe tremor. Finally, Class 4 was made up of healthy subjects without any neurological impairments. (Figure 2.5).

ID	SEX	AGE	SIDE	EDSS	9-HPT	BBT	TREMOR	CLINICAL CLASS
S1	M	29	R	1	20.43	66	NO	1
S2	F	38	R	1.5	15.53	71	NO	1
S3	F	39	R	4.5	42.28	31	YES	2
S4	M	39	R	2	25.30	49	NO	1
S5	F	38	L	-	24.70	42	NO	2
S6	M	34	R	3.5	23.50	52	NO	1
S7	M	35	R	1	17.60	59	NO	1
S8	F	64	L	6.5	NE	12	YES	3
S9	F	63	L	6.5	66.34	33	YES	2
SS	M/F	28:60	L/R	-	-	-	-	4

Figure 2.5: Clinical overview of subjects recruited: in green PwMS clinically classified as Class 1 (without tremor), in red PwMS clinically classified as Class 2 (with moderate tremor or other cerebellar impairments), in white PwMS clinically classified as Class 3 (with severe tremor), in yellow healthy subjects clinically classified as Class 4.

All participants performed a specific pick-and-place task on the transversal plane using Microsoft HoloLens 2 technology and ROCKapp.

Prior to participating, all individuals provided written consent after receiving information about the research. The study adhered to ethical standards outlined in the Declaration of Helsinki. The research protocol, labeled as "IIT REHAB HT01 (363/2022) - DB id 12494", received approval from the Ethical Committee of Liguria Region in Genoa, Italy.

In essence, the study aimed to obtain metrics from healthy subjects' dataset, compute these metrics for MS patients, and then compare their performances to obtain a classification while maintaining ethical conduct and adhering to established guidelines.

2.3   Experimental Setup and Protocol

The ROCKapp task was conducted in a seated position to accommodate individuals with significant lower limb impairments. Each experimental session lasted

approximately 30 minutes, with a minimum 1-hour interval between subjects for recharging the Hololens 2 battery.

The MR environment of ROCKapp was developed as a tool for assessing upper limb (UL) functional abilities, focusing on pick-and-place tasks relevant to daily activities. Visual cues were incorporated to prompt interaction with physical objects, facilitating their movement between locations and unlocking rewards upon accurate object placement.

ROCKapp targeted UL movements in the transversal plane, requiring participants to maneuver physical objects to various holographic targets.

Upon launching the application on the HoloLens 2, users selected their dominant hand (right or left) using buttons from the MRTK library.

Initiation of the task presented users with a holographic target where a 500 ml physical bottle was to be positioned. Tracking was facilitated by a cylindrical PTC Vuforia marker attached to the bottle cap, enabling comprehensive tracking from all angles (Figure 2.6).

Figure 2.6: ROCKapp setup: user point of view on top, user viewed from outised on the bottom picture

Participants were instructed to follow four cardinal cues—front close (S), front distant (N), left (W), and right (E)—to encourage specific arm trajectories. Virtual

target N was set at maximum arm extension, while S, W, and E formed vertices of a 28 cm square. Position N served as the reference point for returning the bottle after movement to S, W, or E, with the order of cue appearances randomized. Placing the object on an activated target triggered the launch of a holographic rocket.

Each participant completed the task 30 times across 5 trials, with each trial comprising 6 movements (Figure 2.7).
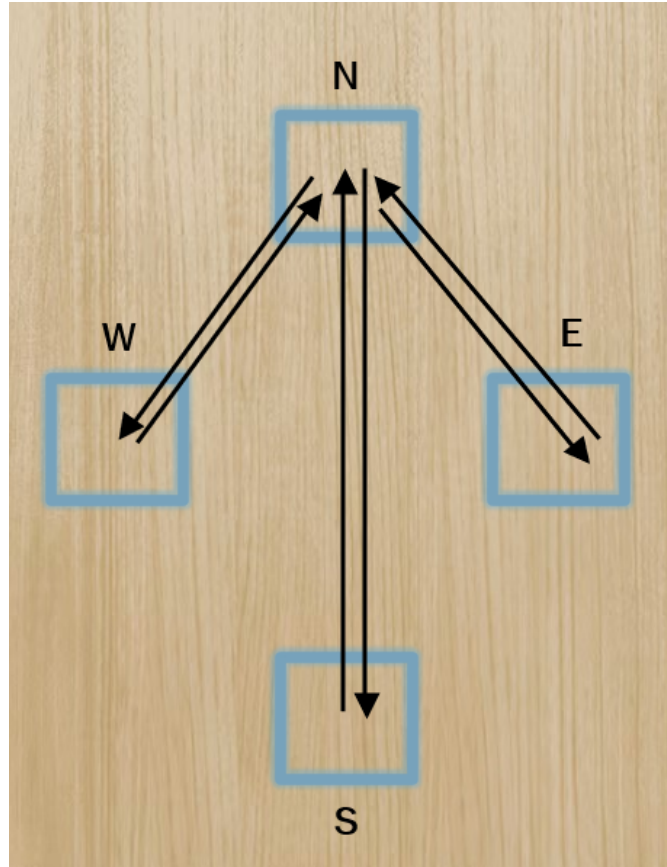
Figure 2.7: Position of targets visualized through HoloLens2 and movements directions.

2.3.1 Experimental Protocol

1. Participants were welcomed into the experimental setting and provided informed consent for participation. They then donned the Hololens 2 device.

2. Ocular calibration was performed because the distance from which the user visualizes markers during this process can impact their recognition and spatial

placement, potentially causing a discrepancy between the intended and actual positions of clues. To mitigate this issue, the application is designed so that calibration is required only once by the user. This approach ensures that the user consistently perceives the clues in the same location. Furthermore, ocular calibration provides accurate visual-motor data essential for analyzing eye-hand coordination. This personalized calibration process enhances both the accuracy and reliability of clue placement and the assessment of eye-hand coordination.

3. Participants were instructed to execute movements in a natural manner to simulate ADL. Specifically, they were required to grasp a bottle and place it on an illuminated target positioned in one of the four cardinal directions on the table. After releasing the bottle, they had to position their hand at rest on the side corresponding to their dominant hand, either right or left. They would then retrieve the bottle once more and transfer it to the next illuminated target. This sequence of actions was repeated to ensure a thorough simulation of ADL.

4. Participants were instructed to maintain the bottle's position within the field of view of the Hololens 2 at all times to ensure continuous data capture.

5. Subsequently, the application was initiated, marking the beginning of the experimental session.

6. Following the completion of the exergame session, participants were requested to complete a comprehensive 15-question multiple-choice questionnaire designed to evaluate their engagement levels and the degree of stress induced by the rehabilitation activity.

2.4 Preprocessing

Hand- and eye-tracking data recorded from HoloLens 2 were gathered into a text file for subsequent processing. In Unity, a fixed framerate of 50 Hz was applied to ensure consistency, and data were saved at this frequency. During gameplay, ROCKapp generated a detailed log file that captured the necessary information. These log files were then converted into Excel files, which were structured in a specific format to facilitate further analysis and visualization. The Excel files were structured as follows, allowing for easy manipulation and examination of the recorded data:

- **Hand-tracking data**: Contains information about hand and bottle movements, positions, and interactions with virtual targets, divided into 18 coloumns

1. Experiment date in dd/mm/yyyy format

2. Time of frame acquisition in hh:mm:ss format

3. (

4. Start movement point of the bottle: -1 if it's the first movement and the subject needs to bring the bottle to the reference position (N), otherwise indicates 0 for N, 1 for E, 2 for S, or 3 for W

5. -

6. End movement point of the bottle: it indicates 0 for N, 1 for E, 2 for S, or 3 for W

7.)

8. Instantaneous x-coordinate of the hand

9. Instantaneous y-coordinate of the hand

10. Instantaneous z-coordinate of the hand

11. – "Area": indicates if the position coincides with a hand-bottle collision with the target,
    – otherwise empty.

12. – "Target": indicates if the position coincides with a hand-bottle collision with the target,
    – "Bottle" if the hand and bottle colliders are in collision but not with a target,
    – otherwise empty.

13. – One of the 4 cardinal points (N, S, E, W) if the position coincides with a hand-bottle collision with the target,
    – "Grabbed" if the hand and bottle colliders are in collision but not with a target,
    – otherwise empty.

14. Empty column

15. "Bottle_Position"

16. Target bottle position x-coordinate

17. Target bottle position y-coordinate

18. Target bottle position z-coordinate

The following table shows an example of one possible Excel Hand-tracking disposition [Table 2.1].

Table 2.1: Excel Hand-Tracking Disposition - The subject is doing a movement from S to N and the hand and the bottle are in the N Target Area.

Date	21/11/2023
Time	09:25:45
Parenthesis	(
Start Coord	2
Minus sign	-
End Coord	0
Parenthesis	)
Hand x	0.706674
Hand y	-0.7676431
Hand z	0.2886219
Area	Area
Collision	Target
Cardinal	N
Empty	
Bottle Position	Bottle_position
Bottle x	0.7290909
Bottle y	-0.671493
Bottle z	0.308109

- **Eye-tracking data**: Includes data on gaze direction and gaze origin during the tasks, divided into 25 columns:

  1. Experiment date in dd/mm/yyyy format

  2. Time of frame acquisition in hh:mm:ss format

  3. (

  4. Start movement point of the bottle: -1 if it's the first movement and the subject needs to bring the bottle to the reference position (N), otherwise indicates 0 for N, 1 for E, 2 for S, or 3 for W

  5. -

  6. End movement point of the bottle: it indicates 0 for N, 1 for E, 2 for S, or 3 for W

  7.)

8. "Gaze"

9. "dir"

10. Instantaneous x-coordinate of the gaze direction

11. Instantaneous y-coordinate of the gaze direction

12. Instantaneous z-coordinate of the gaze direction

13. "Gaze"

14. "orig"

15. Instantaneous gaze origin x-coordinate

16. Instantaneous gaze origin y-coordinate

17. Instantaneous gaze origin z-coordinate

18. – "Area_Target": indicates if the position coincides with a hand-bottle collision with the target,
    – otherwise empty.

19. – "Area": indicates if the position coincides with a hand-bottle collision.
    – otherwise empty.

20. – "Target": indicates if the position coincides with a hand-bottle collision,
    – "Bottle" if the hand and bottle colliders are in collision but not with a target,
    – otherwise empty.

21. – One of the 4 cardinal points (N, S, E, W) if the position coincides with a hand-bottle collision with the target,
    – "Grabbed" if the hand and bottle colliders are in collision but not with a target,
    – otherwise empty.

22. "Bottle_Position"

23. Target bottle position x-coordinate

24. Target bottle position y-coordinate

25. Target bottle position z-coordinate

The following table shows an example of one the corresponding Excel Eye-tracking disposition to the previous Excel Hand-tracking one [Table 2.2].

This conversion facilitated further data analysis and statistical processing required for the study.

Table 2.2: Excel Eye-Tracking Disposition - The subject is doing a movement from S to N and the hand and the bottle are in the N Target Area.

Date	21/11/2023
Time	09:25:45
Parenthesis	(
Start Coord	2
Minus sign	-
End Coord	0
Parenthesis	)
Gaze	Gaze
dir	dir
Gaze dir x	-0.1543665
Gaze dir y	-0.5797307
Gaze dir z	-0.8000522
Gaze	Gaze
origin	origin
Gaze origin x	0.743416
Gaze origin y	-0.4229481
Gaze origin z	0.6713781
Area_Target	Area_Target
Area	Area
Collision	Target
Cardinal	N
Bottle Position	Bottle_Position
Bottle x	0.7290909
Bottle y	-0.671493
Bottle z	0.308109

2.4.1 Data Transfer and Struct Creation

The initial step involves transferring these Excel files from the HoloLens 2 to the MATLAB environment. This transfer guarantees that the data is accessible for subsequent manipulation and analysis using MATLAB's advanced data processing capabilities. Once the data has been imported into MATLAB, it is organized into a struct, divided by subjects (from S1 to S21). To facilitate data analysis, the first movement from the random position -1 to the reference point N is removed as it cannot be standardized.

2.4.2 Handling Missing Values

HoloLens 2 occasionally fails to detect the hand, resulting in "-100" values in the x, y, and z coordinates of the hand in the dataset. These erroneous values were replaced with "NaN" values (Not a Number) to indicate missing data points. To preserve data integrity, linear interpolation was applied to estimate these missing values.

2.4.3 Rototranslation of data

As a first step, rototranslation was performed on the data to transform the left-handed coordinate system of Hololens2 to a standard right-handed coordinate system.

Subsequently, the centroid positions of Target Areas N and S were computed from the Hand dataset by averaging all x and y coordinates corresponding to rows where column 13 of the Hand-Tracking dataset indicated 'S' or 'N'. To establish a unified reference system across all subjects, the centroid of Target Area N was translated to the position (0;0), aligning with the origin of the coordinate system, and all dataset points were rigidly translated accordingly. Subsequently, considering the line connecting centroid N to centroid S, the angle of inclination of this segment relative to the y-axis was calculated, and a rigid rotation of the dataset around the z-axis was performed to nullify the NS segment's inclination relative to the y-axis. This procedure standardized the dataset, ensuring comparability across all data points.

2.4.4 Filtering Position and Velocity Data

The 3D positional data of the hand and the bottle were processed separately to compute the absolute position using the formula:

$$position = \sqrt{X^2 + Y^2 + Z^2}$$

A 6-Hz cutoff fourth order low-pass Butterworth filter was applied to the trajectories to reduce noise [35].

Similarly, the velocity of the hand movements was calculated using the formula:

$$velocity = \sqrt{V_x^2 + V_y^2 + V_z^2}$$

A 2-Hz cutoff fourth order low-pass Butterworth filter was applied to the trajectories to smooth out the data and remove high-frequency noise components.

2.4.5   Movements Manual Segmentation

After calculating the absolute positions and velocities for each subject, the actual collision points with the N, S, E, and W targets were identified by imposing thresholds on the x and y coordinates. These thresholds reflected the relative positions and distances between the targets as defined by the experimental setup. By visually inspecting the absolute positions and velocities over time, in conjunction with the positions of the markers identified on their respective signals, the most suitable cut-off points for isolating individual movements performed by the subjects were determined. During this phase of preprocessing, manual segmentation enabled a rough separation of the movements, including a portion of the final "reach to grasp" phase and an initial portion of the "return to resting position" phase.

2.5   Data Processing

Once the individual movements were isolated, they were organized into a structure that facilitated data organization. Reflecting the initial data segmentation, the data were divided by subject, encompassing a total of 12 healthy subjects and 9 PwMS. This subject-wise division prepared the data for subsequent comparisons both between the two participant groups and among subjects within the same group. Each movement was then further divided into repetitions, with each movement corresponding to 5 repetitions as outlined by the experimental protocol. This data segmentation allowed for a subsequent analysis to understand the repeatability and consistency of each patient's movements across the repetitions of the same movement. Position and Velocity values were computed again, but this time only the 6-Hz cutoff fourth order low-pass Butterworth filter was applied to the trajectories, to preserve the main components of the velocity profile.

2.5.1   Physiological Interpolation

The dataset described in the previous paragraph then underwent a new phase of data interpolation at the points where HoloLens 2 had failed to detect the signal. To allow for a more realistic interpolation of the data, a 5th-degree polynomial was used [36].

2.5.2   Minimum Velocity Points Identification

In order to segment the actual pick-and-place movement of the object, excluding the "reach to grasp" and "return to resting position" phases, an algorithm for automatic movement segmentation was implemented. Specifically, this algorithm relies on identifying velocity minima to isolate the peak corresponding to the actual

movement, from the moment the subject grasps the bottle to the moment it is placed on the target. Specifically, only the first minimum within the first quarter of the signal and the last minimum within the last quarter of the signal were considered for segmentation. This approach ensures that essential phases of the movement are not excluded.

2.5.3 Movements Exclusion Criteria

Before segmenting the movements, the percentage of undetected points (NaN) by HoloLens 2 was calculated to determine if there were signals unsuitable for analysis. It was found that subject S2 had an overall NaN percentage exceeding 80%, demonstrating its unusability. Therefore, it was excluded from the analysis.

Once a dataset containing the actual movements was obtained and organized hierarchically by subjects, movements, and repetitions, the signals underwent individual analysis. At this stage, the dataset comprised a total of 531 movements.

Initially, signals containing more than 25% undetected points by HoloLens 2 were excluded to ensure they accurately represented the performed movements, without significant distortions or artifacts introduced by interpolation.

Following this analysis, subject S14 was also excluded from the analysis because it exhibited a NaN percentage exceeding 25% in the majority of movements (90% of available movements). Using this method, excluding subject 14, 3.77% of the available dataset was discarded.

Finally, through visual analysis of individual movements, all movements with distorted morphology unsuitable for our study purposes were removed. This step resulted in an additional 24.27% of the available dataset being eliminated to effectively analyze only undistorted real data.

2.6 Metrics and Statistical Analysis

This master's thesis focuses on analyzing motor control and coordination during upper-limb movements in people with multiple sclerosis (PwMS). To achieve a more precise assessment, the analysis concentrated on a specific movement phase, excluding irrelevant segments. This approach allowed the extraction of a dataset that served as the basis for computing various kinematic metrics.

These kinematic metrics were instrumental in quantifying the quality and efficiency of movement execution, providing valuable insights into the motor performance of PwMS during rehabilitation exercises. The use of the selectively extracted dataset ensured that the computed metrics accurately reflected the characteristics of the targeted movement phase, thereby enhancing the relevance and validity of the analysis. Specifically, the study selected several kinematic metrics related

to hand and eye displacements and velocities, focusing on smoothness, efficiency, morphology and hand-eye coordination [33, 35].

2.6.1 Smoothness

- **Spatial Arc Length (SPARC)**: SPARC is defined as the Arch Length of the frequency spectrum derived from the Fourier Transform of the velocity profile.

  This metric is inverted, meaning that more negative values indicate less smooth movements. SPARC is recognized as a crucial measure of upper-limb impairments because of its reliability in assessing movement smoothness.

$$\text{SPARC} = -\int_{f_{\min}}^{f_{\max}} \left| \mathcal{F}\left\{\frac{dv(t)}{dt}\right\} \right|^2 dt$$

- **Number of Velocity Peaks (NVP)**: NVP denotes the number of submovements required to complete an action. Hand motion patterns showing multiple peaks in the velocity curve signify impaired smoothness, while a bell-shaped velocity profile is characteristic of normal, healthy movement.

  This metric is employed to quantify neurological recovery, as a reduction in the number of submovements indicates enhanced motor control [37].

$$h_i \geq \frac{1}{2} \cdot h_{\max}$$

  where $h_{\max}$ is the maximum peak height. Additionally, peaks were required to be separated from any preceding peak by a distance (di) of at least 5% of the total path length (L):

$$d_i \geq 0.05 \times L$$

2.6.2 Efficiency

- **Movement Time (MT)**: MT is defined as the duration of the movement from the moment the object is picked to when it is placed on the target.

  It is widely associated with the overall efficiency of the movement.

$$\text{MT} = t_{\text{end}} - t_{\text{start}}$$

2.6.3 Morphology

- **Symmetry**: Symmetry measures the similarity between the two halves of a movement and offers insights into coordination and balance. For patients in rehabilitation, particularly those recovering from conditions like stroke or MS, Symmetry is a crucial indicator of recovery progress.

  Clinically, high Symmetry in movements indicates effective motor control and suggests proper functioning of the patient's neuromuscular system [38]. In contrast, movement asymmetry can signify motor impairments or compensatory strategies, potentially necessitating further therapeutic intervention.

$$\text{Symmetry} = \frac{\text{Duration of the Acceleration Phase}}{\text{Duration of the Deceleration Phase}}$$

- **Kurtosis**: Kurtosis offers insights into the distribution of velocity throughout a movement. High Kurtosis indicates that the movement features more frequent extreme values (peaks), while low Kurtosis suggests a more consistent distribution of velocities.

  Clinically, Kurtosis can aid in evaluating the smoothness and control of a patient's movements. Higher Kurtosis values may point to abrupt or jerky motions, which are often associated with motor control issues or neurological disorders. Conversely, lower Kurtosis values suggest smoother and more controlled movements.

2.6.4 Hand-Eye Coordination

- **Gaze Accuracy Number of Zero Crossing Points (N0C_GA)**: Gaze accuracy, calculated as the distance between the eye path and the hand path instantaneously, refers to the measurement of how closely the gaze trajectory follows the hand trajectory at each moment in time. It quantifies the spatial correspondence between where the eyes are looking and where the hand is moving throughout a movement. This metric is crucial in understanding the precision and alignment of eye-hand coordination during motor tasks or behavioral studies.

  In this study, we chose to present this metric by calculating the number of zero crossing points of the first derivative of the distance between the eye path and the hand path (N0C_GA). This approach provides a quantitative measure of how often the gaze trajectory intersects or deviates from the hand trajectory over time. By analyzing the derivative's zero crossings, we can capture changes in gaze accuracy dynamically throughout the task or experimental session. This method enhances our ability to detect subtle fluctuations in eye-hand

coordination and offers a detailed assessment of the temporal smoothness of gaze accuracy [35]. Such analysis is valuable for uncovering patterns of motor control and potentially identifying impairments or variations in sensorimotor integration across different conditions or populations.

- **Pearson's Coefficient**: The Pearson's Correlation Coefficient, also known as Pearson's r, is a measure of the linear correlation between two variables X and Y. It quantifies the strength and direction of the linear relationship between the variables. The Pearson's Correlation Coefficient is defined as the covariance of the two variables divided by the product of their standard deviations [26].

$$r = \frac{\text{cov}(\text{hand\_displacement}, \text{eye\_displacement})}{\text{std}(\text{hand\_displacement}) \cdot \text{std}(\text{eye\_displacement})}$$

This formula captures the degree to which the two absolute displacements are linearly related, with values ranging from -1 to 1.

$$1 \geq r \geq -1$$

From a clinical perspective, the correlation between eye and hand movements allows for the assessment of coordination between ocular and upper limb movements, which may be impaired in cases of cerebellar dysfunction. Correlation values approaching 1 indicate that eye movements accurately follow hand movements. Negative correlation values indicate an inverse relationship between eye and hand movements, while values approaching zero suggest a lack of synchronization between the two pathways, both indicative of non-physiological behavior.

2.7 Clustering Methods

After calculating the aforementioned metrics individually for each MS-affected patient and the mean value of all the healthy subjects, the obtained values were clustered using 4 methods to identify common behavioral patterns across different disease severities. Subjects were grouped into four classes across all clustering methods:

- **Class 1**: MS subjects without cerebellar impairments

- **Class 2**: MS subjects with moderate tremor and other cerebellar impairments

- **Class 3**: MS subjects with severe tremor

- **Class 4**: Healthy subjects or MS subjects exhibiting behavior similar to that of healthy individuals

The analyses were conducted in two distinct ways:

- **Metric-by-Metric Clustering**: Each metric was analyzed separately using the four clustering methods.

- **Normalized Multi-Metric Clustering**: All metrics were normalized with respect to the mean value of healthy subjects for each metric and then aggregated to cluster the subjects using the four methods.

The following sections briefly outline the clustering methods chosen for the analysis:

2.7.1   K-means

The K-means algorithm is a widely used partitioning technique in the field of data clustering. The following steps outline the process executed by the K-means algorithm:

1. **Initialization**: Select the number of clusters, K, and initialize K cluster centroids.

2. **Assignment Step**: Assign each data point to the nearest cluster centroid. This is typically achieved by calculating the Euclidean distance between each data point and each centroid, then assigning the data point to the cluster associated with the nearest centroid.

3. **Update Step**: Recalculate the centroids of each cluster. The new centroid is computed as the arithmetic mean of all data points assigned to that cluster, thereby updating its position.

4. **Iteration**: Repeat the assignment and update steps until the centroids stabilize, meaning they no longer change significantly. Convergence can be assessed by checking if the changes in centroids are below a predefined threshold or if a maximum number of iterations is reached [39].

The K-means algorithm offers several key advantages, including simplicity, computational efficiency, and scalability to large datasets. The algorithm's time complexity is $O(nkl)$, where n is the number of data points, k is the number of clusters, and l is the number of iterations required for convergence.

Nevertheless, K-means has some limitations. It is sensitive to the initial placement of centroids, which can affect the final clustering results. Additionally,

determining the optimal number of clusters can be challenging. The algorithm also struggles with clusters of varying sizes and densities. Despite these limitations, K-means remains a fundamental and widely-used clustering method due to its ease of implementation and effectiveness in a variety of practical applications.

2.7.2 Affinity Propagation

Affinity Propagation is a clustering algorithm that identifies exemplars within a dataset by simultaneously considering all data points as potential exemplars. Unlike traditional clustering methods that require predefining the number of clusters, Affinity Propagation does not need a priori specification of cluster numbers, making it particularly useful in scenarios where the optimal number of clusters is unknown or variable.

The algorithm operates by iteratively exchanging messages between data points to determine both exemplars and cluster assignments. Each data point evaluates the suitability of all others as its exemplar based on a similarity measure, typically defined by a similarity matrix. The message passing process involves two types of messages: "responsibility" messages, which quantify how well-suited a data point is to be an exemplar for another, and "availability" messages, which reflect the attractiveness of a data point to choose another as its exemplar.

Through iterative message exchanges, data points update their preferences for exemplars and adjust their cluster memberships until a stable set of exemplars and clusters is achieved. The algorithm converges when the assignments of exemplars and clusters no longer change significantly between iterations [40].

Affinity Propagation is known for its ability to discover clusters of varying sizes and densities, as well as its capability to handle large datasets efficiently. However, its sensitivity to the initial setting of parameters, such as the damping factor that controls message updates, requires careful tuning to achieve optimal results. Additionally, while Affinity Propagation can be computationally intensive, its flexibility and robustness make it suitable for applications in diverse scientific fields, including biology, computer vision, and social network analysis.

2.7.3 Agglomerative Clustering

Agglomerative clustering is a fundamental bottom-up technique in data analysis and machine learning used to group similar objects into clusters hierarchically. The process begins by considering each data point as its own cluster and then iteratively merging clusters based on a measure of similarity until all data points belong to a single cluster or a stopping criterion is met.

Initially, each data point is treated as a separate cluster. The algorithm then proceeds by iteratively merging the two closest clusters based on a specified distance

metric, such as Euclidean distance or correlation coefficient. This merging process continues until all the data points are grouped into a single cluster.

Agglomerative clustering operates under the principle of linkage criteria, which determines how the distance between clusters is measured and how clusters are merged. Common linkage criteria include:

- **Single linkage**: Merging clusters based on the minimum distance between their closest members.

- **Complete linkage**: Merging clusters based on the maximum distance between their farthest members.

- **Average linkage**: Merging clusters based on the average distance between all pairs of members from different clusters.

Agglomerative clustering is valued for its simplicity and interpretability, as well as its ability to handle a wide range of data types and cluster shapes. However, its computational complexity can be a limiting factor for large datasets, especially when employing distance computations for all pairs of clusters. Despite this challenge, agglomerative clustering remains widely used in various scientific and practical applications due to its intuitive nature and ability to reveal hierarchical relationships within data [41].

2.7.4 Divisive Clustering

Divisive clustering, also known as top-down clustering, represents an alternative approach to hierarchical clustering compared to agglomerative methods. In divisive clustering, the process begins with all data points (or documents) in a single cluster at the top level. The cluster is then recursively split into smaller clusters using a flat clustering algorithm, such as K-means, until each data point resides in its own individual cluster [39].

This top-down approach contrasts with the bottom-up nature of agglomerative clustering, where clusters are progressively merged. Divisive clustering is conceptually more intricate because it necessitates an additional flat clustering algorithm as a subroutine to perform the splits. However, it offers advantages in efficiency when only a limited number of hierarchical levels need to be generated, as it can be linear in terms of the number of documents and clusters.

One of the distinguishing characteristics of divisive clustering is its hierarchical rigidity. Once a split is made, it cannot be undone, which simplifies computation by avoiding the need to explore all possible combinations. This rigidity can lead to lower computational costs but necessitates careful consideration of clustering quality enhancement techniques to optimize results.

Chapter 3

Results

In this section, a comprehensive analysis of kinematic profiles is presented, providing an in-depth examination of specific motor control deficits in patients with MS and evaluating the potential of targeted rehabilitation strategies to enhance motor function. This analysis not only quantifies the extent of impairment but also enhances the understanding of altered motor control mechanisms in neurodegenerative diseases.

In this study, the kinematic profiles of hand position and velocity during the pick-and-place motor task were analyzed for both healthy subjects and MS patients (Figure 3.1a, 3.1b, 3.2a, 3.2b). The data were analyzed to quantify the impairments in motor control in MS patients by comparing them with the results obtained from the analysis of healthy subjects' movements.

To quantify motor control alterations, various metrics were calculated from position and velocity profiles to identify specific patterns in hand kinematics and assess the level of eye-hand coordination. Specifically, the following characteristics of hand movements were evaluated: homogeneity, efficiency, and morphology [Table 3.1]. For eye-hand coordination, the assessment was based on the relationship between hand and gaze positions relative to the subject [Table 3.2].

Performance	Metric	Abbreviation	Reference
Smoothness	Spatial Arc Length	SPARC	[42, 35, 43]
Smoothness	Number of Velocity Peaks	NVP	[42, 43]
Efficiency	Movement Time	MT	[42, 44, 45]
Morphology	Symmetry	-	[46]
Morphology	Kurtosis	-	[46]

Table 3.1: Five kinematic features were selected according to three different hand movement performance evaluations: smoothness, efficiency and morphology. Abbreviations are reported, as well as literature references, if present.

Performance	Metric	Abbreviation	Reference
Hand-Eye Coordination	Gaze Accuracy Number Of Zero Crossing Points	N0C_GA	-
Hand-Eye Coordination	Pearson Coefficient	r	[26]

Table 3.2: Two different features were selected based on the assessment of hand-eye coordination. Abbreviations are reported, as well as literature references, if present.

3.1 Kinematic Analysis

Participants were instructed to perform six consecutive movements, three outward and three return, during a motion capture analysis (acquisition frequency of 50 Hz). The pick-and-place task involved grasping a bottle from one of the cardinal points visualized by a blue hologram and moving it to the next blue hologram. This next hologram was located at another cardinal point. The outward movement always started from the North cardinal point and ended at a different cardinal point, distinct from the endpoints of the other outward movements. Each return movement always concluded at the North cardinal point.

Each sequence was subjected to five repetitions, with no restrictions on timing or pathways. Participants were asked to perform the task in a relaxed and natural manner.

Figures 3.1a and 3.1b, show the aligned and superimposed positions of the subjects for each movement. Each subplot of the movement contains all repetitions except those deemed unusable.

Specifically, in Figure 3.1a the aligned and superimposed positions of all healthy subjects are shown. In Figure 3.1b, the positions of subjects with MS without tremor are shown in blue, while the positions of patients with tremor (S3, S8, and S9), as well as S5, who, despite not exhibiting tremor, had a high degree of impairment, are shown in red.

The total number of movements depicted in Figure 3.1a is 223, while the total movements present in Figure 3.1b is 183.

Figures 3.2a and 3.2b show the corresponding aligned, superimposed, and normalized velocities of the subjects' positions under examination.
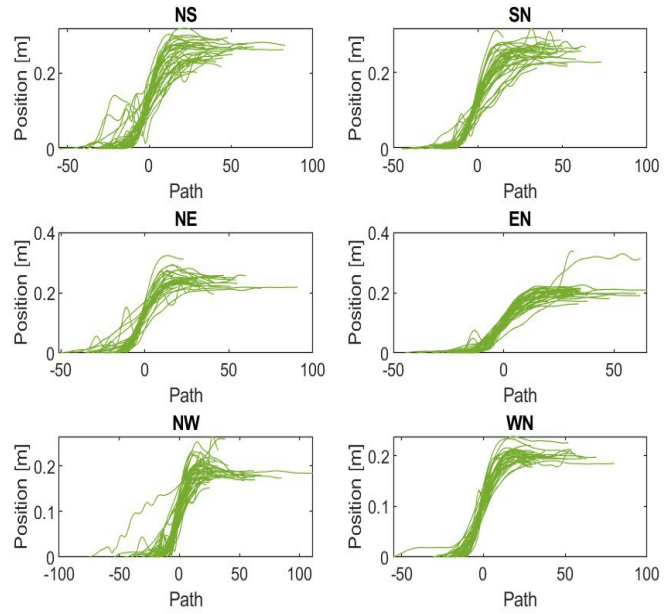
(a) Green: Positions of healthy subjects.
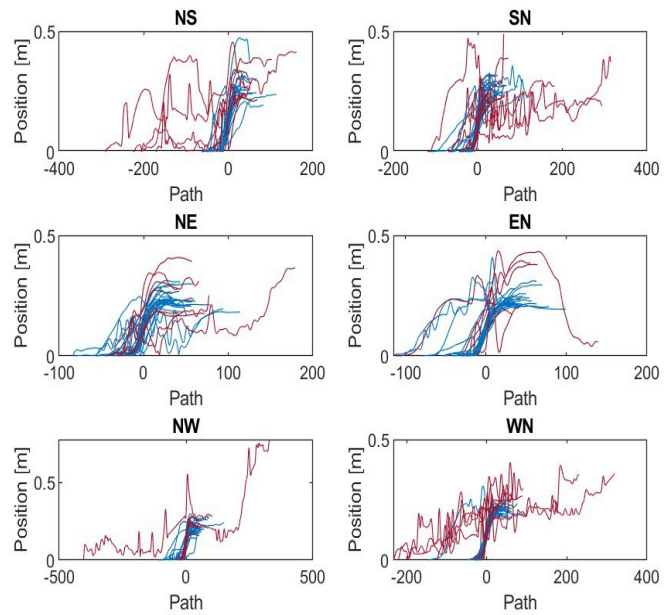
(b) Blue: positions of subjects with MS without tremor, red: positions of subjects with MS with tremor and of S5 who does not have tremor but has other cerebellar impairments.

Figure 3.1: Positions of all overlapped repetitions for each movement: (a) positions of the healthy subjects (b) positions of PwMS.
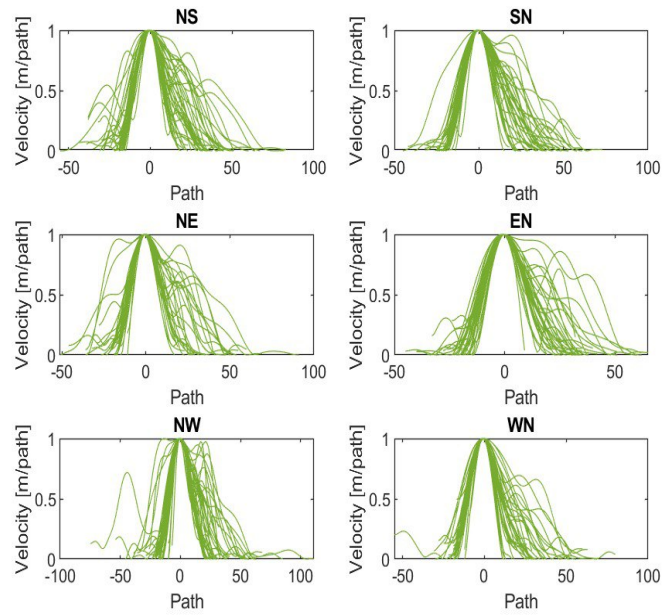
(a) Green: velocities of healthy subjects.
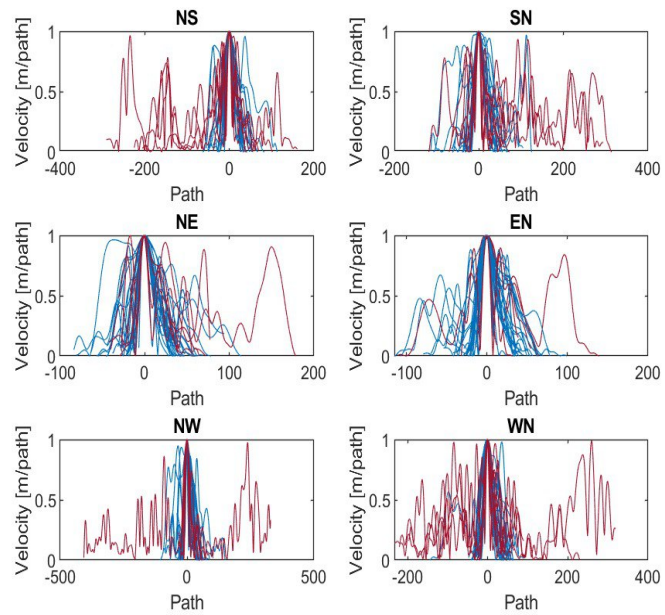
(b) Blue: velocities of PwMS without tremor, red: velocities of PwMS with tremor and of S5 who does not have tremor but has other cerebellar impairments.

Figure 3.2: velocities of all overlapped repetitions for each movement: (a) velocities of the healthy subjects (b) velocities of PwMS.

Positions and corresponding velocities are analyzed, and metrics are calculated. Healthy subjects are considered as a single entity by averaging across all subjects, repetitions, and movements to obtain a single value for each movement. Subsequently, the results of the metrics for patients with MS are presented and compared with the results for healthy subjects, who are represented as an average of all values for each individual metric.

In particular, in Figures 3.3, 3.5, 3.7, 3.9 and 3.11, the box chart of the mean value of the considered metric for healthy subjects is shown in gray along with its standard deviation, calculated by averaging across all movements, repetitions, and healthy subjects. Overlaid on the mean values of the healthy subjects are the metric values for each individual movement and repetition for each patient, with the patient code on the x-axis and the corresponding values on the y-axis.

In Figures 3.4, 3.6, 3.8, 3.10 and 3.12, the metric values for each patient are shown differently. Specifically, for each dot plot corresponding to a patient, the x-axis represents the movement code, and the y-axis represents the corresponding metric value for that movement, averaged across repetitions (orange). The blue shows the metric value corresponding to the movement, averaged across repetitions for all healthy subjects, so the metric values for each dot plot are the same.

3.1.1   Spectral Arc Length

In Figure 3.3, it is observed that most of the SPARC metric values for S1, S4, S6, and S7, who are patients without tremor, are around the mean value. However, patient S5 (a patient without tremor) behaves similarly to patients with tremor such as S3, S8, and S9.

Specifically, most values for S3 and S9 are outside the mean range, while for S8, there are no values around the mean, but only values outside of it.

In Figure 3.4, the first subplot, corresponding to S1, as well as the subplots for S4, S6, and S7, show values similar to the metric values for healthy subjects, except for the NW and WN movements of S1, the NE and EN movements of S4, and the NS movement of S7. The values for these movements slightly deviate from the corresponding values of healthy subjects.

Additionally, the values for S8 (patient with tremor) significantly deviate from the mean values of healthy subjects, being much lower.

43
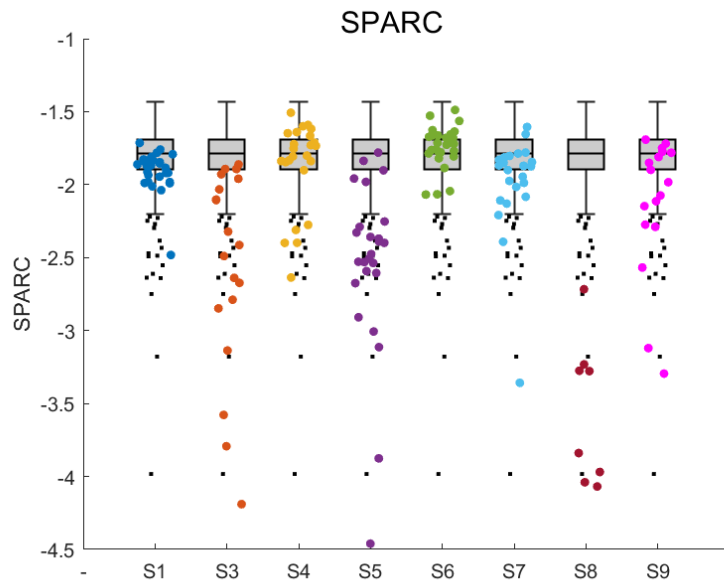
Figure 3.3: Boxchart of SPARC metric: In gray the average and standard deviation of values for healthy subjects; other color: dots represent the values for each motion repetition of pathological subjects, with each patient distinguished by a unique color.
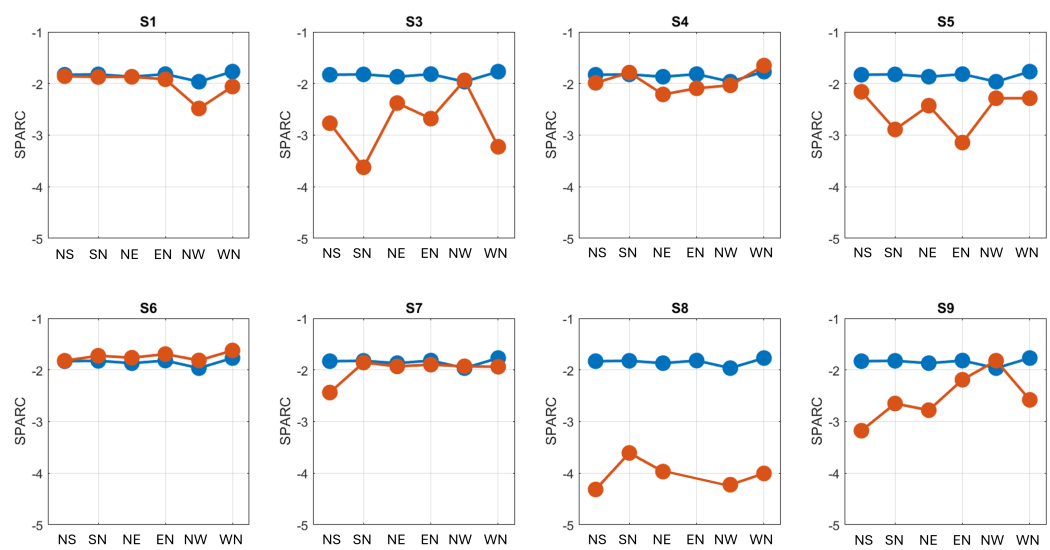
Figure 3.4: Dotplot of SPARC metric: Blue dots represent the mean value across repetitions for each movement in healthy subjects, while orange dots represent the mean value across repetitions for each movement in a pathological subject.

44

3.1.2 Number of Velocity Peaks

In Figure 3.5, it is observed that patients with MS without tremor, particularly S4 and S6, have a number of velocity peaks ranging between 1 and 5, which is lower than the range observed in healthy subjects. Subject 1 shows values between 1 and 7, and S7 between 1 and 8. Subject S5, who did not exhibit tremor, has a wider range of values, similar to patients with tremor such as S8. On the other hand, S3 also has a wider range of values compared to patients without tremor but still lower than S8. Additionally, S9 has a range equal to S7 but still lower than S1.

In Figure 3.6, it is noted that S8 deviates significantly from both patients without tremor, other patients with tremor, and healthy subjects, having a wider range of values compared to the others. Moreover, for S4 and S6, the range of values is similar to that of healthy subjects and differs from all other patients, both those without tremor and those with tremor.

Figure 3.5: Boxchart of NVP metric: In gray the average and standard deviation of values for healthy subjects; other color: dots represent the values for each motion repetition of pathological subjects, with each patient distinguished by a unique color.

Figure 3.6: Dotplot of NVP metric: Blue dots represent the mean value across repetitions for each movement in healthy subjects, while orange dots represent the mean value across repetitions for each movement in a pathological subject.

3.1.3 Movement Time

In Figure 3.7, the MT metric values of patients without tremor, S1 and S4, overlap with the mean and standard deviation of healthy subjects. Most values of S7 (a patient without tremor) also overlap with the standard deviation of healthy subjects, with a few values slightly higher. Patients with tremor, particularly S3, S5, and S9, exhibit some values higher than healthy subjects, while none of the values for subject S8 overlap with the mean and standard deviation of healthy subjects. In fact, its values are much higher compared to both healthy subjects and all other subjects with MS.

Similarly, in Figure 3.8, it is observed that the metric value for individual movements corresponding to S8 significantly deviates from the mean of healthy subjects, showing much higher values compared to both healthy subjects and other subjects with MS. Other patients with tremor, S3 and S9, show values that differ and do not overlap with healthy subjects except for the NW movement of S3, which is similar to the mean value across all repetitions for healthy subjects in the same movement.

Additionally, for patients S4 and S6, the values are similar to those of healthy subjects and differ from all other patients, both those without tremor and those with tremor.

Figure 3.7: Boxchart of MT metric: In gray the average and standard deviation of values for healthy subjects; other color: dots represent the values for each motion repetition of pathological subjects, with each patient distinguished by a unique color.
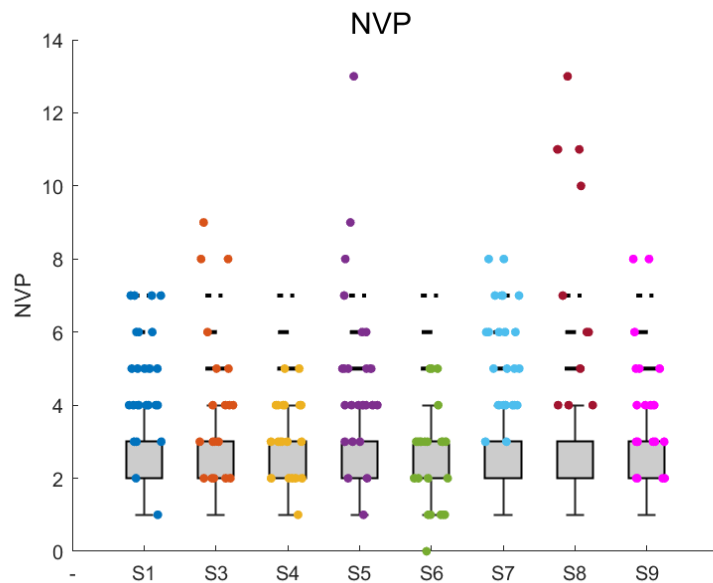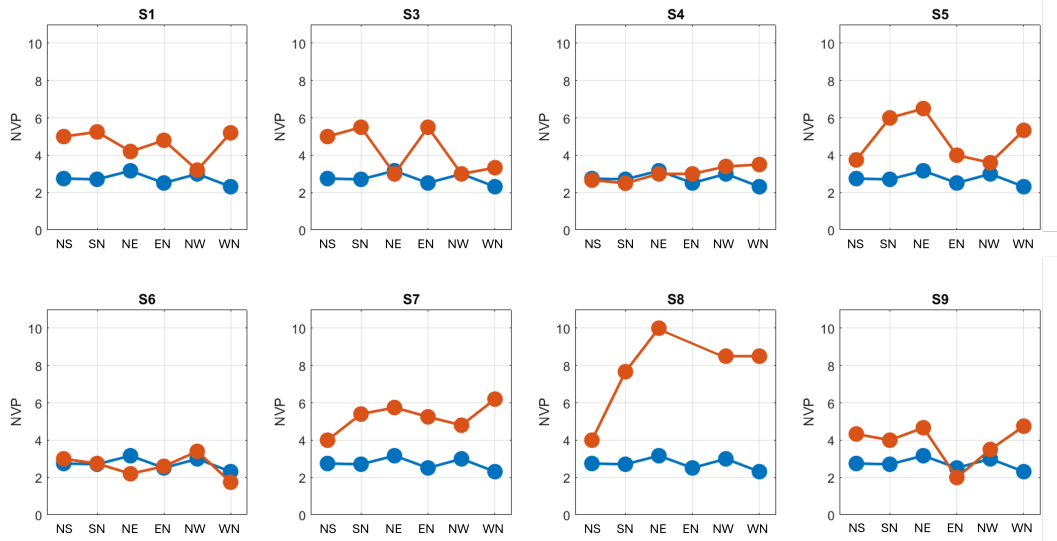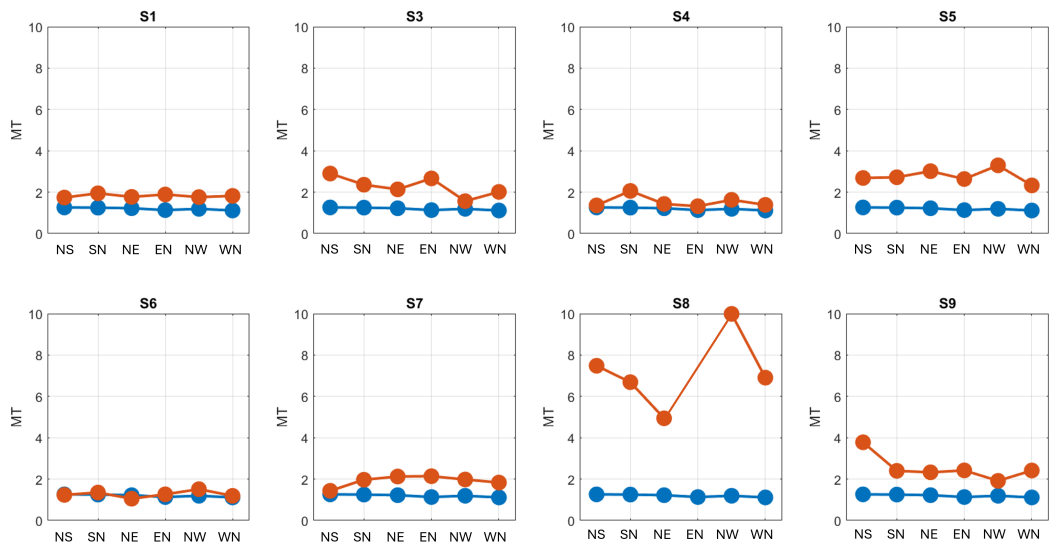

Figure 3.8: Dotplot of NVP metric: Blue dots represent the mean value across repetitions for each movement in healthy subjects, while orange dots represent the mean value across repetitions for each movement in a pathological subject.

47

3.1.4   Symmetry

In Figure 3.9, it is observed that for patients without tremor, namely S1, S4, S6, and S7, most Symmetry metric values fall within the mean and standard deviation of healthy subjects' metric values. However, subject S8 (a patient with tremor) and subject S5 (a patient without tremor) exhibit values outside the mean and standard deviation of healthy subjects, notably higher in magnitude. Similarly, subjects S3 and S9 (both patients with tremor) show values outside the mean and standard deviation of healthy subjects, notably lower in magnitude.

In Figure 3.10, it is noted that the value of the Symmetry metric for individual movements of patients S4, S6, and S7 (patients without tremor) is similar to the value of the corresponding movement averaged across all repetitions for healthy subjects, except for the SN movement of subject S4 and the NS movement of subject S7, which deviate significantly from the corresponding movement value of healthy subjects.

The values for subject S8 significantly deviate from those of healthy subjects. Additionally, the value corresponding to the EN movement for subject S5 (a patient without tremor) deviates significantly from the corresponding value of the movement in healthy subjects, being higher.

Figure 3.9: Boxchart of Symmetry metric: In gray the average and standard deviation of values for healthy subjects; other color: dots represent the values for each motion repetition of pathological subjects, with each patient distinguished by a unique color.
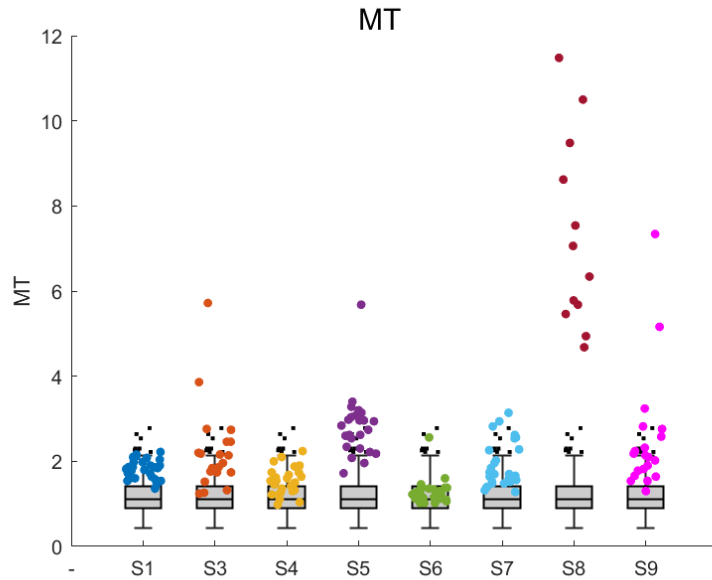
Figure 3.10: Dotplot of Symmetry metric: Blue dots represent the mean value across repetitions for each movement in healthy subjects, while orange dots represent the mean value across repetitions for each movement in a pathological subject.

3.1.5 Kurtosis

In the Figure 3.11, it is shown that most Kurtosis metric values for subjects with MS without tremor, specifically S1, S4, S6, and S7, fall within the mean and standard deviation of healthy subjects' metric values, except for patient S5, whose values are outside the mean and standard deviation of healthy subjects. This pattern is also observed in patients S3, S8, and S9, who had tremors. Particularly, S8's values are entirely outside the mean and standard deviation of healthy subjects' metric values, except for one value from a single repetition.

In Figure 3.12, it is noted that the Kurtosis metric value for individual movements of patients without tremor, S1, S6, and S7, is similar to the value of the corresponding movement averaged across all repetitions for healthy subjects, except for the NS movement of patient S7, which slightly deviates from the corresponding movement value of healthy subjects, particularly being higher. Additionally, all values for S4 (patient without tremor) deviate slightly from the values of healthy subjects, especially the SN movement.

The values for patients with tremor (S3, S8, S9) deviate more significantly from the values of healthy subjects, with S8's values notably higher overall, except for the NE movement, which is similar to the metric value of the corresponding movement in healthy subjects. Furthermore, S5, a patient without tremor, also

shows significantly different values compared to both healthy subjects and other patients without tremor.

Figure 3.11: Boxchart of Kurtosis metric: In gray the average and standard deviation of values for healthy subjects; other color: dots represent the values for each motion repetition of pathological subjects, with each patient distinguished by a unique color.
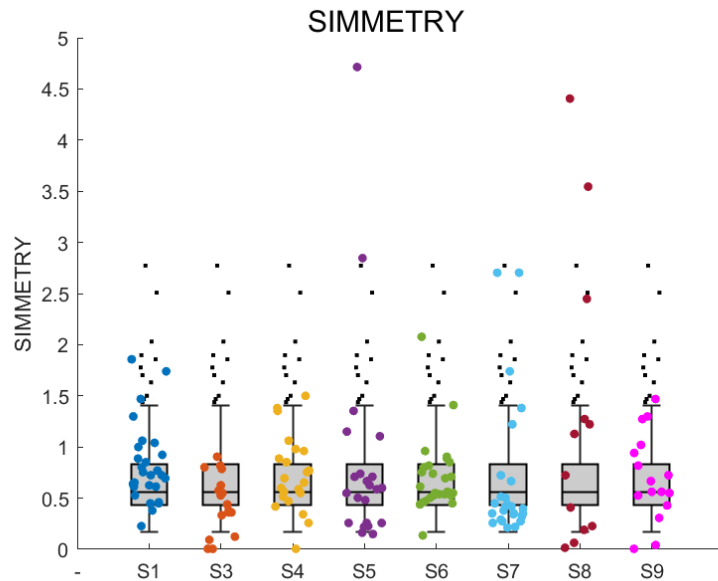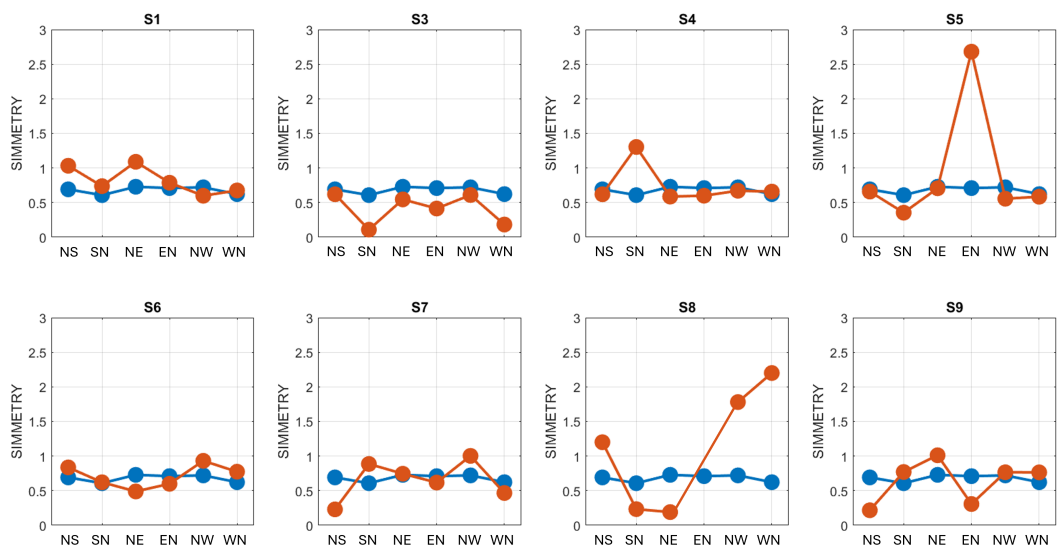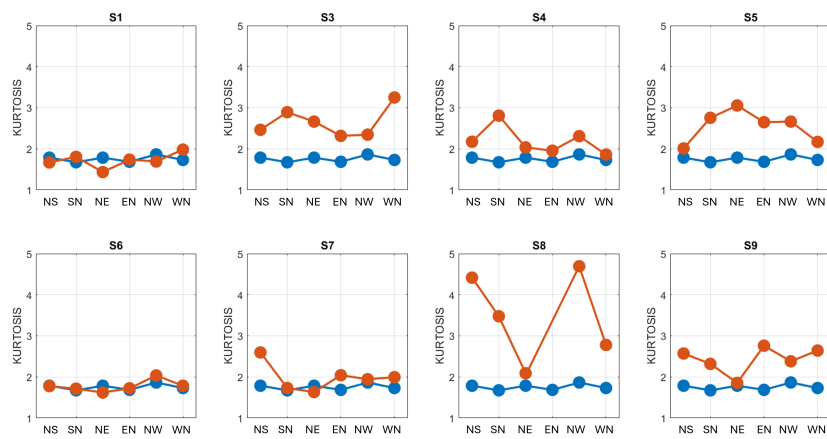

Figure 3.12: Dotplot of Kurtosis metric: Blue dots represent the mean value across repetitions for each movement in healthy subjects, while orange dots represent the mean value across repetitions for each movement in a pathological subject.
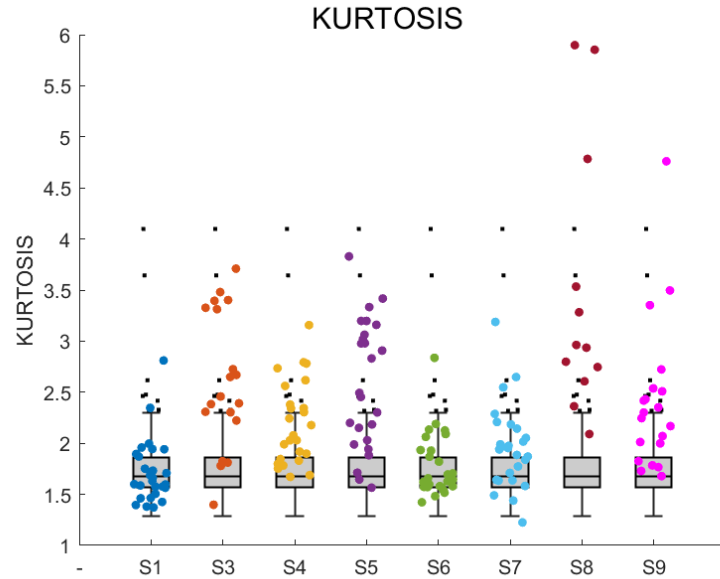
3.2   Hand-Eye Coordination

Another important aspect, in addition to the kinematic one, is eye-hand coordination. To quantify coordination, hand movement positions are compared with eye positions for each subject using two different metrics: Gaze Accuracy Number Of Zero Crossing Points (N0_GA) and the Pearson Coefficient.

Subsequently, in Figures 3.13 and 3.15, the results of these 2 metrics are shown for each multiple sclerosis patient, comparing them with results from healthy subjects.

Specifically, for the N0C_GA metric, in Figure 3.13, the box plot of the mean value of the metric for healthy subjects is shown in gray, along with its standard deviation calculated by averaging across all movements, repetitions, and healthy subjects. Overlaying this are the values of the metric for each movement of each repetition for each subject, plotted with patient codes on the x-axis and corresponding values on the y-axis.

In Figure 3.14, the metric values for each patient are displayed differently. Particularly, each patient's dot plot shows the movement code on the x-axis and the corresponding metric value averaged over repetitions (in orange). The metric values averaged over all healthy subjects for each movement are shown in blue, ensuring consistency across all dot plots.

The Pearson coefficient, calculated as the ratio of covariance between hand and eye positions to the product of their standard deviations, ranges from -1 to 1: values nearing 1 indicate a linear relationship between hand and corresponding eye movement, null values indicate independence between the two variables, while values approaching -1 indicate an inverse linear relationship, indicating poor eye-hand coordination in some cases.

The Pearson coefficient (Figure 3.15) is calculated individually for each multiple sclerosis patient for each movement by averaging across repetitions. Conversely, a single Pearson coefficient is calculated for each movement for all healthy subjects, averaging across both repetitions and the number of healthy subjects.

Values of -1 are represented in blue, while values of 1 are represented in green; thus, values between -1 and 1 exhibit varying shades of color from blue to green.

3.2.1   Gaze Accuracy Number of Zero Crossing Point

In Figure 3.13, it is shown that most N0C_GA metric values for multiple sclerosis patients without tremor, specifically S1, S4, S6, and S7, fall within the mean and standard deviation of healthy subjects' metric values, except for patient S5, whose values are outside the mean of healthy subjects, as well as values from S3 and S8, patients with tremor. Particularly, S8's values are entirely outside the mean and

standard deviation of healthy subjects' metric values. Additionally, the metric values for subject S9, who had tremor, mostly fall within the mean and standard deviation of healthy subjects.

In Figure 3.14, for the majority of cases, the N0C_GA metric value for individual movements of subjects S1, S4, S6, and S7 (patients without tremor) appears similar to the value of the corresponding movement averaged across all repetitions for healthy subjects, except for the NW movement of subject S6 and the EN movement of subject S7, both of which slightly deviate from the value of the corresponding movement of healthy subjects, particularly being higher.

Most values for subjects with tremor (S3, S8, S9) deviate more significantly from the values of healthy subjects, with S8's values notably higher overall, indicating a significant deviation. Furthermore, S5, a patient without tremor, also shows significantly different values compared to both healthy subjects and other patients without tremor.
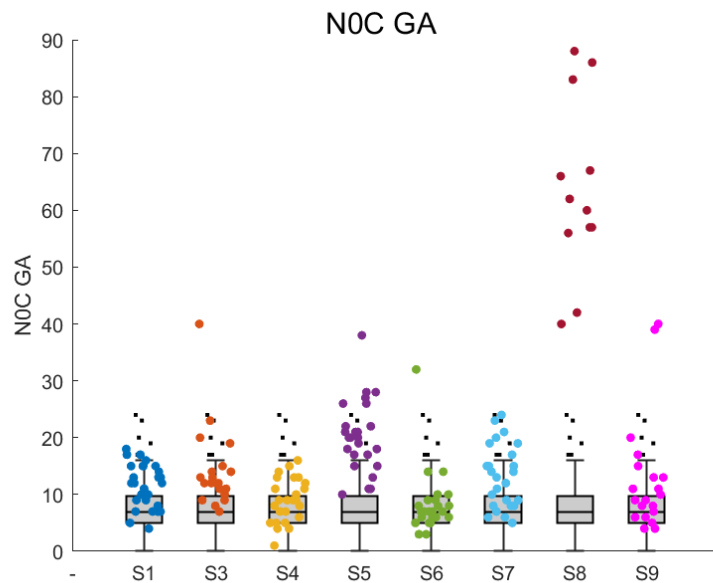
Figure 3.13: Boxchart of N0C_GA metric: In gray the average and standard deviation of values for healthy subjects; other color: dots represent the values for each motion repetition of pathological subjects, with each patient distinguished by a unique color.
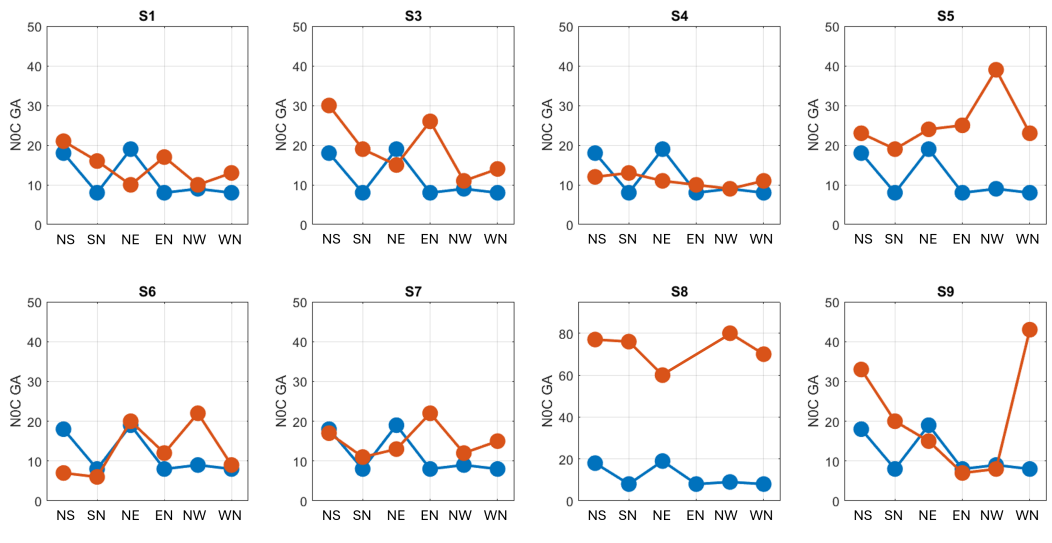
Figure 3.14: Dotplot of N0C_GA metric: Blue dots represent the mean value across repetitions for each movement in healthy subjects, while orange dots represent the mean value across repetitions for each movement in a pathological subject.

3.2.2 Pearson's Coefficient

In Figure 3.15, it is observed that for some MS patients, the Pearson's coefficient value is negative, such as for movement SN of S3 and movement WN of S5. Additionally, for S5, the coefficient value for movement NE is positive but very close to 0.

However, it is noted that MS patients generally have values above 0.6 and approaching 1. Specifically, certain values stand out, such as the coefficient for movement NS of S1, S6, S8, and S9, movement SN of S1, S5, S6, and S7, movement NE of S1, S8, and S9, movement EN of S7, movement NW of S8 and S9, and the coefficient for movement WN of S4, S6, and S9.

Moreover, in some cases, pathological subjects' values are higher compared to the mean of healthy subjects, particularly notable for the coefficient of movement NS for S1, S3, S6, S8, and S9, movement SN for S1, S5, S6, and S7, movement NE for S8 and S9, movement EN for S7, movement NW for all pathological subjects except S1, S2, and S4, and finally, the Pearson's coefficient value for movement WN corresponding to S3, S5, and S9.

	S1	S3	S4	S5	S6	S7	S8	S9	SANI
NS	0,8543	0,5606	0,3939	0,2033	0,8084	0,273	0,6264	0,6338	0,4278
SN	0,8173	-0,00459	0,2734	0,6149	0,6323	0,622	0,1898	0,3732	0,5416
NE	0,6822	0,4924	0,6087	0,06118	0,3532	0,2788	0,7098	0,8286	0,6936
EN	0,2891	0,2832	0,4334	0,4217	0,4247	0,6986	–	0,3775	0,523
NW	0,2758	0,319	0,5055	0,2016	0,5168	0,5658	0,7076	0,8328	0,4005
WN	0,5741	0,5641	0,7849	-0,08934	0,704	0,5177	0,6004	0,7082	0,61
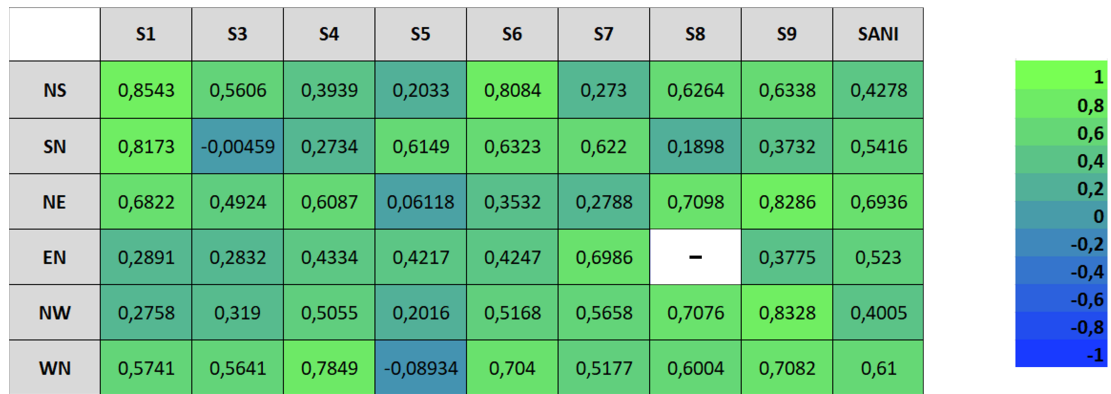
Figure 3.15: Pearson's coefficient for each movement for each subject with MS and Pearson's coefficient for each movement for all healthy subjects.

3.3 Clustering results

Following the calculation of the specified metrics for each patient with MS individually and the mean values for all healthy subjects, the resulting data were clustered using four distinct methods to identify common behavioral patterns across various levels of disease severity. The subjects were categorized into four classes using all clustering techniques:

- **Class 1**: MS subjects without cerebellar impairments

- **Class 2**: MS subjects with moderate tremor and other cerebellar impairments

- **Class 3**: MS subjects with severe tremor

- **Class 4**: Healthy subjects or MS subjects exhibiting behavior similar to that of healthy individuals

The analyses were conducted in two distinct ways:

- Metric-by-Metric Clustering

- Normalized Multi-Metric Clustering

Each cell in each table in Figures 3.16, 3.17, 3.18 and 3.19, shows the classification class for a specific subject for a specific metric with different colors representing each class: red for class 1, green for class 2, white for class 3, and yellow for class 4; While each cell in Figure 3.20 shows the classification class for a specific subject according to the second method of analysis (Normalized Multi-Metric Clustering).

54

3.3.1 Metric-by-Metric Clustering

Each metric was analyzed separately using the four clustering methods.

Figure 3.16 shows the results obtained using K-means Clustering, Figure 3.17 presents the results from Affinity Propagation clustering, Figure 3.18 illustrates the results from Agglomerative Clustering, and the final figure (Figure 3.19) displays the results from Divisive clustering.

In all clustering methods, healthy subjects are classified into class 4.

For the K-means clustering (Figure 3.16), using the mean values of each metric as input, averaged across all movements and repetitions for each subject, the following classification was obtained:

- **For the SPARC metric**: Class 1 includes patients S1, S4, and S7, Class 2 includes patients S3, S5, and S9, Class 3 includes patient S8, and Class 4 includes patient S6.

- **For the NVP metric**: Class 1 includes patients S1, S5, and S7, Class 2 includes patients S3 and S9, Class 3 includes patient S8, and Class 4 includes patients S4 and S6.

- **For the MT metric**: Class 1 includes patients S1, S3, and S7, Class 2 includes patients S5 and S9, Class 3 includes patient S8, and Class 4 includes patients S4 and S6.

- **For the SYMMETRY metric**: Class 1 includes patients S1 and S5, Class 2 includes patient S3, Class 3 includes patient S8, and Class 4 includes patients S4, S6, S7, and S9.

- **For the KURTOSIS metric**: Class 1 includes patients S4 and S7, Class 2 includes patients S3, S5, and S9, Class 3 includes patient S8, and Class 4 includes patients S1 and S6.

K-MEANS CLUSTERING					
	SPARC	NVP	MT	SIMMETRY	KURTOSIS
S1	1	1	1	1	4
S3	2	2	1	2	2
S4	1	4	4	4	1
S5	2	1	2	1	2
S6	4	4	4	4	4
S7	1	1	1	4	1
S8	3	3	3	3	3
S9	2	2	2	4	2
SS	4	4	4	4	4

Figure 3.16: Classification accordingly k-means clustering.

Using Affinity Propagation Clustering (Figure 3.17), the following classification was obtained:

- **For the SPARC metric**: Class 1 includes patient S3, Class 2 includes patients S1, S5, and S9, Class 3 includes patient S8, and Class 4 includes patients S4, S6, and S7.

- **For the NVP metric**: Class 1 includes patients S1, S5, and S7, Class 2 includes patients S3 and S9, Class 3 includes patient S8, and Class 4 includes patients S4 and S6.

- **For the MT metric**: Class 1 includes patients S3, S4, and S6, Class 2 includes patients S5 and S9, Class 3 includes patient S8, and Class 4 includes patients S1 and S7.

- **For the SYMMETRY metric**: Class 1 includes patients S1, S6, and S7, Class 2 includes patients S5 and S9, Class 3 includes patients S3 and S8, and Class 4 includes patient S4.

- **For the KURTOSIS metric**: Class 1 includes patients S4 and S5, Class 2 includes patients S3, S7, and S9, Class 3 includes patient S8, and Class 4 includes patients S1 and S6.

AFFINITY PROPAGATION CLUSTERING					
	SPARC	NVP	MT	SIMMETRY	KURTOSIS
S1	2	1	4	1	4
S3	1	2	1	3	2
S4	4	4	1	4	1
S5	2	1	2	2	1
S6	4	4	1	1	4
S7	4	1	4	1	2
S8	3	3	3	3	3
S9	2	2	2	2	2
SS	4	4	4	4	4

Figure 3.17: Classification accordingly Affinity Propagation clustering.

Using Agglomerative Clustering (Figure 3.18), the following classification was obtained:

- **For the SPARC metric**: Class 1 includes patients S1, S4, and S7, Class 2 includes patients S3, S5, and S9, Class 3 includes patient S8, and Class 4 includes patient S6.

- **For the NVP metric**: Class 1 includes patients S1, S5, and S7, Class 2 includes patients S3 and S9, Class 3 includes patient S8, and Class 4 includes patients S4 and S6.

- **For the MT metric**: Class 1 includes patients S1 and S7, Class 2 includes patients S3, S5, and S9, Class 3 includes patient S8, and Class 4 includes patients S4 and S6.

- **For the SYMMETRY metric**: Class 1 includes patients S1 and S5, Class 2 includes patient S3, Class 3 includes patient S8, and Class 4 includes patients S4, S6, S7, and S9.

- **For the KURTOSIS metric**: Class 1 includes patients S4 and S7, Class 2 includes patients S3, S5, and S9, Class 3 includes patient S8, and Class 4 includes patients S1 and S6.

AGGLOMERATIVE CLUSTERING					
	SPARC	NVP	MT	SIMMETRY	KURTOSIS
S1	1	1	1	1	4
S3	2	2	2	2	2
S4	1	4	4	4	1
S5	2	1	2	1	2
S6	4	4	4	4	4
S7	1	1	1	4	1
S8	3	3	3	3	3
S9	2	2	2	4	2
SS	4	4	4	4	4

Figure 3.18: Classification accordingly Agglomerative clustering.

Using Divisive Clustering for each subject for each metric (Figure 3.19) was obtained the same classification obtained by using Agglomerative Clustering.

DIVISIVE CLUSTERING					
	SPARC	NVP	MT	SIMMETRY	KURTOSIS
S1	1	1	1	1	4
S3	2	2	2	2	2
S4	1	4	4	4	1
S5	2	1	2	1	2
S6	4	4	4	4	4
S7	1	1	1	4	1
S8	3	3	3	3	3
S9	2	2	2	4	2
SS	4	4	4	4	4

Figure 3.19: Classification accordingly Divisive clustering.

3.3.2   Normalized Multi-Metric Clustering

All metrics were normalized with respect to the mean value of healthy subjects for each metric and then aggregated to cluster the subjects using the four methods.

In Figure 3.20, each cell shows the classification class for a specific subject for a specific clustering method.

In all clustering methods, healthy subjects are classified into class 4.

- **For the K-means clustering**: Class 1 includes patients S1, and S7, Class 2 includes patients S3, S5, and S9, Class 3 includes patient S8, and Class 4 includes patients S4 and S6.

- **For the Affinity Propagation clustering**: Class 1 includes patient S1, Class 2 includes patients S3, S5 and S9, Class 3 includes patient S8, and Class 4 includes patients S4, S6 and S7.

- **For the Agglomerative clustering**: the classification is the same of K-means clustering.

- **For the Divisive clustering**: the classification is the same of K-means clustering and of Agglomerative clustering.

	K-MEANS	AFFINITY PROPAGATION	AGGLOMERATIVE CLUSTERING	DIVISIVE CLUSTERING
S1	1	1	1	1
S3	2	2	2	2
S4	4	4	4	4
S5	2	2	2	2
S6	4	4	4	4
S7	1	4	1	1
S8	3	3	3	3
S9	2	2	2	2
SS	4	4	4	4

Figure 3.20: Classification accordingly specific clustering method considering Normalized multi-Metric.

Chapter 4

Discussion

Microsoft HoloLens 2, a portable head-mounted display designed for mixed-reality applications, has gained traction in healthcare settings, including surgical robotics [47, 48], elderly assistance [49, 50], and rehabilitation [34]. This study explores its potential for upper-limb functional rehabilitation through a pick-and-place task, offering a promising alternative to expensive and time-consuming motion analysis solutions, particularly in assessing hand movement patterns during ADL recovery.

The study focuses on extracting kinematic features from hand and eye movement patterns captured by the HoloLens 2. Five metrics were selected to assess different aspects of hand trajectories: Symmetry and Kurtosis for morphology, SPARC and NVP for smoothness, and MT for efficiency. Additionally, eye-hand coordination was evaluated using the Pearson Coefficient and N0C_GA.

These metrics were then analyzed using clustering methods to classify subjects into four distinct impairment levels, including healthy individuals for comparative analysis.

In the following sections, the metrics used to evaluate upper limb functionality in individuals with MS will be discussed, and these metrics will be compared with those calculated on the kinematic trajectories of healthy subjects. Additionally, there will be a section discussing the classification of subjects, comparing it with their medical records to verify the insights provided by our method and to see if our classification aligns with the results obtained from clinical tests.

4.1 Smoothness

Analysis of movement smoothness reveals notable distinctions among individuals with impairments, characterized by less fluid movements with frequent abrupt changes in speed. This observation emphasizes the inherent challenges these

individuals encounter in maintaining continuous and controlled movement, crucial for effective rehabilitation.

In MS patients without cerebellar impairments, movement metrics often mirror those of healthy individuals, suggesting preserved motor pathways and coordination mechanisms unaffected by cerebellar lesions. As a result, these individuals typically exhibit smooth and controlled movements, similar to healthy controls.

Specifically, the SPARC metric, in Figures 3.3 and 3.4, serves as a quantitative indicator, demonstrating more negative values in subjects with severe impairments. This signifies increased movement irregularity, indicating difficulties in achieving smooth and consistent movements. SPARC therefore provides critical insights into evaluating the effectiveness of rehabilitation interventions aimed at enhancing movement fluidity.

Conversely, subjects with severe cerebellar impairments display a higher NVP (Figures 3.5, 3.6). This metric indicates frequent speed variations and disjointed movements, highlighting impaired motor coordination and control often seen in patients with cerebellar dysfunction.

When comparing MS patients with and without cerebellar impairments, those with cerebellar dysfunction exhibit more pronounced irregularities in movement patterns, as evidenced by higher NVP values and more negative SPARC values. These differences underscore the significant impact of cerebellar function on movement coordination and control in MS patients.

4.2 Efficiency

The MT metric provides valuable insights into movement efficiency, revealing significant differences between various subject groups (Figures 3.7, 3.8). In subjects with cerebellar impairments, prolonged and variable MT indicates challenges in motor coordination and efficiency during task execution. These individuals often demonstrate irregular acceleration and deceleration patterns, which further impact movement efficiency.

An in-depth analysis of MT underscores its critical role in assessing motor control capabilities and movement precision during daily activities. Optimizing MT within MS rehabilitation programs is essential for improving exercise efficacy and enhancing overall quality of life. Tailored interventions aimed at addressing specific motor challenges in MS patients can promote greater independence and movement precision.

MS patients without cerebellar impairments typically exhibit MT values similar to healthy individuals, which increase as disability progresses due to MS. This progression underscores the deterioration of motor function despite the absence

of cerebellar involvement. In contrast, MS patients with cerebellar dysfunction display significantly higher MT values and greater variability, reflecting impaired motor coordination and control associated with cerebellar lesions.

4.3   Morphology

The results indicate that subjects with impairments exhibit significantly more irregular hand trajectories compared to healthy individuals, indicative of diminished fine motor control. Healthy subjects, in contrast, demonstrate trajectories that are more linear and direct, reflecting precise and coordinated movements.

Analysis of Symmetry (Figures 3.9, 3.10) and Kurtosis (Figures 3.11, 3.12) of velocity curves further elucidates these findings. Lower symmetry values and higher Kurtosis values are often observed in subjects with cerebellar impairments. Lower Symmetry suggests asymmetrical movement patterns, which can be attributed to motor deficits or compensatory strategies due to cerebellar dysfunction. Higher Kurtosis values indicate more abrupt or jerky motions, which are commonly associated with impaired motor control and neurological disorders affecting cerebellar function.

Conversely, MS patients without cerebellar impairments typically exhibit Symmetry and Kurtosis values similar to those of healthy individuals. This similarity suggests that motor coordination and control mechanisms not directly impacted by cerebellar lesions remain relatively intact in these individuals.

Comparing the results highlights distinct patterns: subjects with cerebellar impairments show more irregular hand trajectories, lower Symmetry, and higher Kurtosis values compared to both healthy individuals and MS patients without cerebellar impairments. This underscores the significant impact of cerebellar function on movement patterns and motor control in individuals with impairments, necessitating tailored rehabilitation approaches to address these specific challenges effectively.

4.4   Oculomotor coordination

The analysis of eye-hand coordination metrics, specifically N0C_GA and r, provides insightful findings regarding the relationship between hand and eye movements.

The higher number of zero crossings in MS patients (Figures 3.13, 3.14), particularly those with cerebellar impairments, is closely linked to the presence of dysfunction in the cerebellum. The cerebellum plays a crucial role in coordinating and refining movements by integrating sensory information and fine-tuning motor commands. When cerebellar function is impaired, as often seen in MS patients

with cerebellar lesions or atrophy, there is a disruption in the precision and timing of motor responses. Specifically, N0C_GA indicate changes in the direction of movement coordination between the hand and eye. In healthy individuals and MS patients without significant cerebellar involvement, these crossings tend to occur less frequently and in a smoother manner, reflecting more coordinated and controlled movements. In contrast, MS patients with cerebellar impairments exhibit a higher frequency of zero crossings, indicating more abrupt changes and inconsistencies in the coordination between hand and eye movements. This increased variability and discontinuity can be attributed to the cerebellum's role in error detection and correction during motor tasks. When cerebellar function is compromised, MS patients may experience challenges in accurately predicting and adjusting movements, leading to erratic and less synchronized hand-eye coordination patterns. Therefore, the higher number of zero crossings serves as a quantitative marker of impaired motor coordination, highlighting the specific impact of cerebellar dysfunction in MS on the integration of visual information with motor execution.

On the other hand, in MS patients with significant cerebellar impairments, r may show very low or even negative values (Figure 3.15). This phenomenon can be attributed to the cerebellum's role in fine-tuning motor commands and integrating sensory information. When cerebellar function is compromised, as often occurs in MS patients with cerebellar lesions or atrophy, there is a disruption in the precise synchronization between hand and eye movements. This leads to reduced or inverse correlations between hand and eye positions, reflecting erratic and less coordinated movements.

Conversely, the correlation coefficient r reveals contrasting outcomes. In MS patients, particularly those without cerebellar impairments, r tends to be higher compared to healthy individuals. This higher correlation coefficient suggests that there is a stronger relationship between hand and eye movements, potentially indicating a greater variability or uncertainty in movement execution. This phenomenon may reflect compensatory strategies or adjustments made by MS patients to overcome their neurological challenges while attempting to maintain coordinated movements between the hand and eye. Thus, the variability in r values among MS patients with cerebellar impairments underscores the impact of cerebellar dysfunction on motor coordination. It highlights how neurological deficits affecting the cerebellum can disrupt the integration of visual information with motor actions, resulting in less predictable and less synchronized hand-eye movements compared to both healthy individuals and MS patients without cerebellar involvement.

4.5 Clustering methods

Clinically, the subjects are classified as follows: S1, S4, S6, and S7 in Class 1; S3, S5, and S9 in Class 2; S8 in Class 3; and healthy subjects in Class 4.

The clustering results generally aligned with the clinical data, effectively distinguishing subjects with tremor or cerebellar impairments from both healthy individuals and MS subjects without these impairments. Notably, S8 was set apart from other subjects with cerebellar impairments, exhibiting significantly greater upper limb dysfunction. This distinction underscores the heightened severity of motor impairment in S8, indicating a more profound level of dysfunction compared to other MS subjects with similar cerebellar issues (Figure 3.20). However, some discrepancies were observed:

- S1 and S7: Clinically closer to healthy individuals, as indicated by the best scores in the BBT and the shortest times in the NHPT. However, the clustering methods classified them in Class 1, suggesting they do not exhibit cerebellar impairments but are not perfectly aligned with the behavior of healthy individuals.

- S4 and S6: Clinically classified in Class 1, indicating they do not exhibit cerebellar impairments. Their smooth and well-executed movements in kinematic metrics often led the clustering methods to place them in Class 4, closely aligning their behavior with healthy individuals based on kinematic analysis alone. However, the NHPT and BBT scores for these subjects indicated that their performance differs from that of healthy individuals in clinical assessments. Despite their smooth movements, they may show subtle deficits or inefficiencies that are captured by these clinical tests, leading to their clinical classification as Class 1 rather than Class 4.

This discrepancy underscores the challenge of evaluating upper limb function in MS using only kinematic metrics compared to clinical assessments. While kinematic metrics can capture aspects of movement quality and resemblance to healthy individuals, clinical tests such as the NHPT and BBT provide a more thorough assessment of functional capabilities and specific impairments. Hence, subjects like S4 and S6 may demonstrate similarities to healthy controls in terms of movement fluidity and morphology, yet they may manifest distinct differences in functional performance during clinical evaluations.

Chapter 5

Conclusion

This Master's Thesis explored the usability of Hololens 2 as a tool for assessing upper limb motor control in subjects affected by MS, both with and without cerebellar impairments.

The primary objective of the study was to utilize the hand and eye tracking capabilities of the HoloLens 2 device to compare kinematic data obtained from healthy subjects with those from MS subjects, acquired during a pick and place task in the transverse plane.

The experimental task comprised six different movements delivered in a random order in the four cardinal directions (Figure 2.7). The collected data were subsequently analyzed to extract metrics related to hand-eye coordination, movement morphology, smoothness, and efficiency, aiming to obtain a comprehensive evaluation of movement quality. These results were used to assess both the differences between healthy subjects and those with MS, and to distinguish between MS subjects with and without cerebellar dysfunctions. Comparing metrics from healthy subjects and those with MS allowed to highlight differences in motor control and coordination between the two groups, providing key insights into the impact of MS on upper-limb functionality.

Furthermore, the study aimed to leverage these kinematic metrics to identify distinct motor patterns among all subjects using various clustering methods. The results obtained from clustering techniques divided the subjects into four classes: subjects without tremor, subjects with moderate tremor or other cerebellar impairments, subjects with severe tremor, and healthy subjects or those with a kinematic behavior similar to healthy individuals.

The analysis of movement smoothness revealed significant differences among subjects with impairments, characterized by less fluid movements and frequent

abrupt speed changes. These findings underscored the challenges faced by individuals in maintaining continuous and controlled movement, which are crucial for effective rehabilitation efforts.

In MS patients without cerebellar impairments, movement metrics values closely resembled those of healthy individuals, suggesting preserved motor pathways and coordination mechanisms unaffected by cerebellar lesions. Consequently, these individuals typically exhibit smoother and more controlled movements similar to healthy controls.

The SPARC metric emerged as a valuable quantitative indicator, showing more negative values in subjects with severe impairments, indicative of increased movement irregularity (Figures 3.3, 3.4). This metric played a critical role in evaluating rehabilitation interventions aimed at enhancing movement fluidity.

Conversely, subjects with severe cerebellar impairments exhibited higher NVP values (Figures 3.5, 3.6), signaling frequent speed variations and disjointed movements that highlighted impaired motor coordination and control associated with cerebellar dysfunction.

The MT metric provided insights into movement efficiency, revealing significant differences between subject groups (Figures 3.7, 3.8). In subjects with cerebellar impairments, prolonged and variable MT indicated challenges in motor coordination and efficiency during task execution, characterized by irregular acceleration and deceleration patterns.

An in-depth analysis of MT underscored its critical role in assessing motor control capabilities and movement precision during daily activities. Optimizing MT within MS rehabilitation programs proved essential for improving exercise efficacy and enhancing overall quality of life.

Subjects with impairments demonstrated significantly more irregular hand trajectories compared to healthy individuals, indicative of diminished fine motor control. In contrast, healthy subjects exhibited more linear and direct trajectories, reflecting precise and coordinated movements.

Analysis of Symmetry (Figures 3.9, 3.10) and Kurtosis (Figures 3.11, 3.12) of velocity curves further elucidated these findings, with lower symmetry and higher Kurtosis values observed in subjects with cerebellar impairments. These metrics pointed towards asymmetrical movement patterns and abrupt motions associated with impaired motor control.

Insights into the relationship between hand and eye movements were derived from the examination of eye-hand coordination metrics, specifically N0C_GA (Figures 3.13, 3.14) and r (Figure 3.15). MS patients, particularly those with cerebellar impairments, exhibit higher zero crossings, indicating disrupted coordination between hand and eye movements attributed to cerebellar dysfunction.

In MS patients with significant cerebellar impairments, r may show very low or even negative values, reflecting the compromised cerebellar function that disrupts the synchronization between hand and eye movements. This disruption leads to decreased or opposite correlations between hand and eye positions, indicating less coordinated movements influenced by cerebellar lesions or atrophy.

The clustering results generally aligned with clinical data (Figure 2.5), effectively distinguishing subjects with tremor or cerebellar impairments from healthy individuals and MS subjects without these impairments, supporting the validity of using kinematic metrics for assessing upper limb functionality in MS subjects.

S8 stood out among others with cerebellar impairments, showing significantly greater upper limb dysfunction. However, discrepancies were noted. Subjects S1 and S7, clinically closer to healthy individuals based on BBT and NHPT scores, were classified in Class 1 by clustering methods, suggesting alignment with healthy behavior in kinematic metrics but not in clinical assessments. Similarly, S4 and S6, categorized clinically as Class 1, demonstrated fluid movements resembling those of healthy individuals but displayed variations in functional performance during clinical evaluation.

These findings underscored the necessity for comprehensive assessment methods that integrated both kinematic analysis and clinical testing, providing a more nuanced understanding of movement impairments in MS crucial for effective clinical management and intervention strategies.

5.1 Limitations

Overall, while this study underscores the strengths of the HoloLens 2 in analyzing upper limb motion for rehabilitation purposes, several limitations in the data acquisition phase warrant careful consideration.

A primary concern is the small sample size of participants, potentially limiting the generalizability of our findings to a broader population of MS patients. With a larger and more diverse sample, more robust and representative results could have been established, encompassing the full spectrum of clinical variability among MS patients, including differences in disease severity, age, and time since diagnosis. Moreover, the variability in clinical conditions among MS patients, which encompasses factors beyond disease severity such as overall health status, cognitive function, and specific motor impairments, may not have been fully captured or controlled in our study. This variability significantly impacts the interpretation of our results and emphasizes the importance of comprehensive patient assessment in future research endeavors.

Additionally, the utilization of advanced technologies such as the HoloLens

2 for measuring upper limb motor control introduces inherent challenges. The specific characteristics and performance capabilities of hand-eye tracking devices can influence the outcomes of kinematic metrics, necessitating further validation and calibration to ensure reliability across different patient profiles. Furthermore, relying on a single virtual marker placed on the middle finger of participants may have obscured data due to variations in how patients gripped the bottle during the exercise. This limitation underscores the importance of enhancing sensor placement strategies in future studies. One potential solution could involve incorporating additional virtual markers on the thumb and index finger. This approach would provide more comprehensive tracking of hand movements and grip dynamics, offering a more detailed analysis of upper limb motor control in MS patients.

Lastly, while kinematic metrics offer detailed insights into upper limb movement patterns, they may not fully capture the broader aspects of daily functional capacity and quality of life influenced by MS. Integrating the detailed analysis facilitated by HoloLens 2 with existing clinical tests holds the promise of yielding a comprehensive understanding of the subject's disability severity and tailoring personalized rehabilitative strategies accordingly.

The increasing popularity of exergames in rehabilitation highlights their ability to engage patients across different age groups more profoundly in their recovery process. By immersing patients in mixed reality environments with technologies like HoloLens 2, exercises become more interactive and engaging, thereby fostering neuroplasticity. This not only aids in predicting neurological recovery following clinical relapses in MS but also plays a crucial role in mitigating the clinical manifestations of the disease. Therefore, the integration of HoloLens 2 and exergames represents a promising advancement in the assessment and treatment of MS rehabilitation.

Addressing these limitations is crucial for advancing the reliability and applicability of motion analysis technologies such as HoloLens 2 in clinical research and practice for MS rehabilitation. This improvement will enhance the capacity to effectively evaluate and manage motor impairments in MS patients, thereby improving their overall quality of life and rehabilitation outcomes. This integrated approach, combining assessment with HoloLens 2 alongside clinical tests, not only boosts therapeutic engagement but also holds potential for enhancing the well-being of individuals navigating the complexities of MS.

5.2 Future Works

An interesting future development could involve designing and programming an Artificial Neural Network that, taking as input the signals related to the positions and velocities of the subject's hand, can extrapolate movement metrics and classify

the subject based on kinematic and oculomotor aspects. This approach could significantly improve the accuracy and efficiency in analyzing motion data, offering a powerful tool for evaluation and diagnosis in clinical and rehabilitation settings.

The first challenge lies in collecting a large and representative dataset of hand position and velocity signals, capable of representing the full spectrum of upper limb impairments that MS patients, with and without cerebellar dysfunctions, may exhibit. Preprocessing steps such as normalization and noise reduction are crucial for providing high-quality input to the Neural Network. Choosing the appropriate Neural Network architecture is also critical. Exploring Recurrent Neural Networks (RNNs) adapted for temporal and spatial data could be beneficial, involving the determination of the number of layers, neurons per layer, and optimal hyperparameters.

Training the Neural Network requires substantial computational power, especially with large datasets. Access to adequate hardware, such as powerful GPUs, and optimization techniques, such as early stopping and regularization, are essential to prevent overfitting. Rigorous cross-validation is necessary to evaluate model performance and ensure it does not overfit the training data. Separate validation and test datasets must be created to measure the model's generalizability.

Ensuring the interpretability of the Neural Network's results is another challenge. In a clinical context, it is crucial that the outcomes can be understood and clearly explained to healthcare professionals. Additionally, for this tool to be genuinely useful, it must be integrated with existing clinical systems and workflows.

While designing a Neural Network for the analysis of motion signals is an ambitious and complex project, it offers significant potential to enhance the efficiency and accuracy in evaluating motor skills. The investment in resources and time is justified by the positive impact this technology could have in rehabilitation and clinical diagnosis.

Bibliography

[1] Edward Robert FW Crossman and PJ Goodeve. «Feedback control of hand-movement and Fitts' Law». In: *The Quarterly Journal of Experimental Psychology* 35.2 (1983), pp. 251–278 (cit. on p. 1).

[2] Sonja E Findlater, Erin L Mazerolle, G Bruce Pike, and Sean P Dukelow. «Proprioception and motor performance after stroke: An examination of diffusion properties in sensory and motor pathways». In: *Human Brain Mapping* 40.10 (2019), pp. 2995–3009 (cit. on p. 1).

[3] Ilse Lamers and Peter Feys. «Assessing upper limb function in multiple sclerosis». In: *Multiple sclerosis journal* 20.7 (2014), pp. 775–784 (cit. on pp. 2, 3).

[4] Richard Bohannon. «Measuring muscle strength in neurological disorders». In: *Fizyoterapi Rehabilitasyon* 16.3 (2005), p. 120 (cit. on p. 2).

[5] John F Kurtzke. «Rating neurologic impairment in multiple sclerosis: an expanded disability status scale (EDSS)». In: *Neurology* 33.11 (1983), pp. 1444–1444 (cit. on p. 3).

[6] Virgil Mathiowetz, Gloria Volland, Nancy Kashman, and Karen Weber. «Adult norms for the Box and Block Test of manual dexterity». In: *The American journal of occupational therapy* 39.6 (1985), pp. 386–391 (cit. on p. 4).

[7] Matteo Menolotto, Dimitrios-Sokratis Komaris, Salvatore Tedesco, Brendan O'Flynn, and Michael Walsh. «Motion capture technology in industrial applications: A systematic review». In: *Sensors* 20.19 (2020), p. 5687 (cit. on pp. 4, 5, 13).

[8] Yunfen Wu, María Ángeles Martínez Martínez, and Pedro Orizaola Balaguer. *Overview of the Application of EMG Recording in the Diagnosis and Approach of Neurological Disorders*. Vol. 10. IntechOpen London, UK, 2013 (cit. on p. 4).

[9] Jo Lane, Huah Shin Ng, Carmel Poyser, Robyn M Lucas, and Helen Tremlett. «Multiple sclerosis incidence: a systematic review of change over time by geographical region». In: *Multiple Sclerosis and Related Disorders* 63 (2022), p. 103932 (cit. on p. 5).

[10] R. Dobson and G. Giovannoni. «Multiple sclerosis – a review». In: *European Journal of Neurology* 26 (1 2018), pp. 27–40. DOI: 10.1111/ene.13819 (cit. on pp. 5, 7, 8).

[11] Fred D Lublin. «Clinical features and diagnosis of multiple sclerosis». In: *Neurologic clinics* 23.1 (2005), pp. 1–15 (cit. on p. 6).

[12] W Ian McDonald et al. «Recommended diagnostic criteria for multiple sclerosis: guidelines from the International Panel on the diagnosis of multiple sclerosis». In: *Annals of Neurology: Official Journal of the American Neurological Association and the Child Neurology Society* 50.1 (2001), pp. 121–127 (cit. on p. 7).

[13] Lauren B Krupp, Luis A Alvarez, Nicholas G LaRocca, and Labe C Scheinberg. «Fatigue in multiple sclerosis». In: *Archives of neurology* 45.4 (1988), pp. 435–437 (cit. on p. 7).

[14] Khaled Mohamed Mohamed Koriem. «Multiple sclerosis: New insights and trends». In: *Asian Pacific Journal of Tropical Biomedicine* 6.5 (2016), pp. 429–440 (cit. on p. 8).

[15] Marvin M Goldenberg. «Multiple sclerosis review». In: *Pharmacy and therapeutics* 37.3 (2012), p. 175 (cit. on p. 8).

[16] Werner Helsen, Peter Feys, Elke Heremans, and Ann Lavrysen. «Eye-hand coordination in goal-directed action: normal and pathological functioning». In: (2010) (cit. on p. 8).

[17] Leticia Tornes, Brittani Conway, and William Sheremata. «Multiple sclerosis and the cerebellum». In: *Neurologic clinics* 32.4 (2014), pp. 957–977 (cit. on pp. 9, 11).

[18] SH Alusi, S Glickman, TZ Aziz, and PG Bain. *Tremor in multiple sclerosis.* 1999 (cit. on p. 9).

[19] Patricia K Oakes, Sindhu R Srivatsal, Marie Y Davis, and Ali Samii. «Movement disorders in multiple sclerosis». In: *Physical Medicine and Rehabilitation Clinics* 24.4 (2013), pp. 639–651 (cit. on pp. 9, 10).

[20] J Keiko McCreary, James A Rogers, and Susan J Forwell. «Upper limb intention tremor in multiple sclerosis: an evidence-based review of assessment and treatment». In: *International journal of MS care* 20.5 (2018), pp. 211–223 (cit. on pp. 9, 10).

[21] Christopher W Hess and Seth L Pullman. «Tremor: clinical phenomenology and assessment techniques». In: *Tremor and other hyperkinetic movements* 2 (2012) (cit. on p. 9).

[22] Andrés Labiano-Fontcuberta and Julián Benito-León. «Understanding tremor in multiple sclerosis: prevalence, pathological anatomy, and pharmacological and surgical approaches to treatment». In: *Tremor and other hyperkinetic movements* 2 (2012) (cit. on p. 9).

[23] Günther Deuschl. «Movement disorders in multiple sclerosis and their treatment». In: *Neurodegenerative disease management* 6.6s (2016), pp. 31–35 (cit. on p. 9).

[24] Maurizio Versino, Orest Hurko, and David S Zee. «Disorders of binocular control of eye movements in patients with cerebellar dysfunction». In: *Brain* 119.6 (1996), pp. 1933–1950 (cit. on p. 11).

[25] Peter Feys, WF Helsen, Ann Lavrysen, Bart Nuttin, and P Ketelaer. «Intention tremor during manual aiming: a study of eye and hand movements». In: *Multiple Sclerosis Journal* 9.1 (2003), pp. 44–54 (cit. on p. 11).

[26] Norali Pernalete, Amar Raheja, Manuel Segura, Dimitrios Menychtas, Tyler Wieczorek, and Stephanie Carey. «Eye-hand coordination assessment metrics using a multi-platform haptic system with eye-tracking and motion capture feedback». In: *2018 40th Annual International Conference of the IEEE Engineering in Medicine and Biology Society (EMBC)*. IEEE. 2018, pp. 2150–2153 (cit. on pp. 11, 35, 40).

[27] Mor Nahum, Hyunkyu Lee, and Michael M Merzenich. «Principles of neuroplasticity-based rehabilitation». In: *Progress in brain research* 207 (2013), pp. 141–171 (cit. on p. 12).

[28] Patricia Sánchez-Herrera-Baeza et al. «The impact of a novel immersive virtual reality technology associated with serious games in Parkinson's disease patients on upper limb rehabilitation: a mixed methods intervention study». In: *Sensors* 20.8 (2020), p. 2168 (cit. on p. 12).

[29] Alicia Cuesta-Gómez, Patricia Sánchez-Herrera-Baeza, Edwin Daniel Oña-Simbaña, Alicia Martínez-Medina, Carmen Ortiz-Comino, Carlos Balaguer-Bernaldo-de-Quirós, Alberto Jardón-Huete, and Roberto Cano-de-la-Cuerda. «Effects of virtual reality associated with serious games for upper limb rehabilitation in patients with multiple sclerosis: Randomized controlled trial». In: *Journal of neuroengineering and rehabilitation* 17 (2020), pp. 1–10 (cit. on p. 12).

[30] Vaidehi Patil, Jyotindra Narayan, Kamalpreet Sandhu, and Santosha K Dwivedy. «Integration of virtual reality and augmented reality in physical rehabilitation: a state-of-the-art review». In: *Revolutions in Product Design for Healthcare: Advances in Product Design and Design Methods for Healthcare* (2022), pp. 177–205 (cit. on p. 12).

[31] Omar Mubin, Fady Alnajjar, Nalini Jishtu, Belal Alsinglawi, and Abdullah Al Mahmud. «Exoskeletons with virtual reality, augmented reality, and gamification for stroke patients' rehabilitation: systematic review». In: *JMIR rehabilitation and assistive technologies* 6.2 (2019), e12010 (cit. on pp. 12, 13).

[32] Ali Alawieh, Jing Zhao, and Wuwei Feng. «Factors affecting post-stroke motor recovery: implications on neurotherapy after brain injury». In: *Behavioural brain research* 340 (2018), pp. 94–101 (cit. on p. 13).

[33] Anna Bucchieri, Federico Tessari, Stefano Buccelli, Elena De Momi, Matteo Laffranchi, and Lorenzo De Michieli. «The impact of gravity on functional movements: kinematic insights and features selection». In: *bioRxiv* (2023), pp. 2023–12 (cit. on pp. 16, 19, 33).

[34] Arrigo Palumbo. «Microsoft HoloLens 2 in medical and healthcare context: state of the art and future prospects». In: *Sensors* 22.20 (2022), p. 7709 (cit. on pp. 16, 60).

[35] Nicolas Bayle, Mathieu Lempereur, Emilie Hutin, Damien Motavasseli, Olivier Remy-Neris, Jean-Michel Gracies, and Gwenaël Cornec. «Comparison of Various Smoothness Metrics for Upper Limb Movements in Middle-Aged Healthy Subjects». In: *Sensors* 23.3 (2023), p. 1158 (cit. on pp. 30, 33, 35, 39).

[36] Clautilde Nguiadem, Maxime Raison, and Sofiane Achiche. «Motion planning of upper-limb exoskeleton robots: a review». In: *Applied Sciences* 10.21 (2020), p. 7626 (cit. on p. 31).

[37] Brandon Rohrer, Susan Fasoli, Hermano Igo Krebs, Richard Hughes, Bruce Volpe, Walter R Frontera, Joel Stein, and Neville Hogan. «Movement smoothness changes during stroke recovery». In: *Journal of neuroscience* 22.18 (2002), pp. 8297–8304 (cit. on p. 33).

[38] Slobodan Jaric. «Changes in movement symmetry associated with strengthening and fatigue of agonist and antagonist muscles». In: *Journal of motor behavior* 32.1 (2000), pp. 9–15 (cit. on p. 34).

[39] T Soni Madhulatha. «An overview on clustering methods». In: *arXiv preprint arXiv:1205.1117* (2012) (cit. on pp. 36, 38).

[40] Delbert Dueck. *Affinity propagation: clustering data by passing messages.* University of Toronto Toronto, ON, Canada, 2009 (cit. on p. 37).

[41] Daniel Müllner. «Modern hierarchical, agglomerative clustering algorithms». In: *arXiv preprint arXiv:1109.2378* (2011) (cit. on p. 38).

[42] Anne Schwarz, Christoph M Kanzler, Olivier Lambercy, Andreas R Luft, and Janne M Veerbeek. «Systematic review on kinematic assessments of upper limb movements after stroke». In: *Stroke* 50.3 (2019), pp. 718–727 (cit. on p. 39).

[43] Majid Hajihosseinali, Saeed Behzadipour, Ghorban Taghizadeh, and Farzam Farahmand. «Direction-dependency of the kinematic indices in upper extremities motor assessment of stroke patients». In: *Medical Engineering & Physics* 108 (2022), p. 103880 (cit. on p. 39).

[44] Logan Clark and Sara Riggs. «VR-based kinematic assessments: Examining the effects of task properties on arm movement kinematics». In: *CHI Conference on Human Factors in Computing Systems Extended Abstracts.* 2022, pp. 1–8 (cit. on p. 39).

[45] Aıda M Valevicius, Quinn A Boser, Ewen B Lavoie, Glyn S Murgatroyd, Patrick M Pilarski, Craig S Chapman, Albert H Vette, and Jacqueline S Hebert. «Characterization of normative hand movements during two functional upper limb tasks». In: *PLoS One* 13.6 (2018), e0199549 (cit. on p. 39).

[46] Alfonso Maria Ponsiglione, Carlo Ricciardi, Francesco Amato, Mario Cesarelli, Giuseppe Cesarelli, and Giovanni D'Addio. «Statistical analysis and kinematic assessment of upper limb reaching task in Parkinson's disease». In: *Sensors* 22.5 (2022), p. 1708 (cit. on p. 39).

[47] Alicia Pose-Díez-de-la-Lastra, Rafael Moreta-Martinez, Mónica García-Sevilla, David García-Mato, José Antonio Calvo-Haro, Lydia Mediavilla-Santos, Rubén Pérez-Mañanes, Felix Von Haxthausen, and Javier Pascau. «HoloLens 1 vs. HoloLens 2: improvements in the new model for orthopedic oncological interventions». In: *Sensors* 22.13 (2022), p. 4915 (cit. on p. 60).

[48] Sungmin Lee, Hoijoon Jung, Euro Lee, Younhyun Jung, and Seon Tae Kim. «A preliminary work: mixed reality-integrated computer-aided surgical navigation system for paranasal sinus surgery using Microsoft HoloLens 2». In: *Computer Graphics International Conference.* Springer. 2021, pp. 633–641 (cit. on p. 60).

[49] Mandy Miller Koop, Anson B Rosenfeldt, Kelsey Owen, Amanda L Penko, Matthew C Streicher, Alec Albright, and Jay L Alberts. «The Microsoft HoloLens 2 provides accurate measures of gait, turning, and functional mobility in healthy adults». In: *Sensors* 22.5 (2022), p. 2009 (cit. on p. 60).

[50] Lorans Alabood and Frank Maurer. «An IoT-based Immersive Smart Home System for Seniors with Neurocognitive Disorders.» In: *EMPATHY@ AVI.* 2022, pp. 15–20 (cit. on p. 60).